On the Early Evolution of Forming Jovian Planets II: Analysis of Accretion and Gravitational Torques

Andrew F. Nelson[1]

Max Planck Institut für Astronomie, Königstuhl 17, D-69117 Heidelberg, Germany

Willy Benz

Physikalisches Institut, Universität Bern, Sidlerstrasse 5, CH-3012 Bern, Switzerland

ABSTRACT

We continue our numerical study of the migration of an already formed proto-Jovian companion embedded in a circumstellar disk. We first study the sensitivity of the planet's migration to its mass accretion rate, and find that the disk can supply a forming planet with mass at an essentially infinite rate ($\sim 1 M_{\rm J}/25$ yr) so that a gap could form very quickly via further dynamical interactions between the planet and remaining disk matter. The accreted matter has less orbital angular momentum than the planet and exerts an effective inward torque, so that inward migration is slightly accelerated. However, if a partial gap is formed prior to rapid accretion, the effective torque is small and its contribution to the migration is negligible. Although the disk can supply mass at a high rate, we show that mass accretion rates faster than $\sim 10^{-4} M_{\rm J}$/yr are not physically reasonable in the limit of either a thin, circumplanetary disk or of a spherical envelope. Planet growth and ultimately survival are therefore limited to the planet's ability to accept additional matter, not by the disk in which it resides.

Large gravitational torques are produced both at Lindblad resonances and at corotation resonances. We compare the torques in our simulations to analytic theories at Lindblad resonances and find that common approximations to the theories predict torques that are a factor ~ 10 or more larger than those obtained from the simulations. Accounting for the disk's vertical structure (crudely modeled in our simulations and the theory with a gravitational softening parameter) and small shifts in resonance positions due to pressure gradients, to disk self gravity and to inclusion of non-WKB terms in the analysis (Artymowicz 1993a) can reduce the difference to a factor $\sim 3 - 6$, but do not account for the full discrepancy. Torques from the corotation resonances that are positive in sign, slowing the migration, contribute 20-30% or more of the net torque on the planet, but are not well resolved and vary from simulation to simulation. A more precise accounting of the three dimensional mass distribution and flow pattern near the planet will be required to accurately specify the torques from both types of resonances in the simulations.

We show that the assumption of linearity underlying theoretical analyses of the interactions at Lindblad resonances is recovered in the simulations with planets with masses below $0.5 M_{\rm J}$, but the assumption that interactions occur only at the resonances may be more difficult to support. Angular momentum transfer occurs over a region of finite width near both Lindblad and corotation resonances. The shape of the disk's response there (due e.g. to local variations in epicyclic frequency) varies from pattern to pattern, making the true position of the resonance less clear. We speculate that the finite width allows for overlap and mixing between resonances and may be responsible for the remainder of the differences between torques from theory and simulation, but whether accounting for such overlap in a theory will improve the agreement with the simulations is not clear.

Subject headings: Planets:Migration, Accretion Disks, Hydrodynamics, Numerical Simulations

In a companion paper (**?**)hereafter Paper I]Jov1, we began a study of the early stages of the migration of a Jovian planet through an accretion disk, using numerical simulations. That work was a study of several important systematic effects that affect the results of numerical simulations and an exploration of a very large parameter space of systems. The parameter study was designed to explore the range of possible systems likely to be encountered during the evolution of real circumstellar disks and to make a number of qualitative comparisons of our results to theory. In this work, we concentrate our study on two of the outstanding issues raised in that work.

The first issue concerns our finding that a planet could not complete a transition to Type II migration, unless it was more massive than $0.3M_{\rm J}$, and that the migration rate was both very rapid and very sensitive to the details of the mass distribution within 1–2Hill radii of the planet. The second issue concerns our finding that the migration rates did not follow the theoretically expected linear dependence on planet mass, but that the ${M_{\rm pl}}^{2/3}$ proportionality predicted for the gap width and based on the same physical model did hold.

We study these two issues through a detailed investigation of mass accretion and of the gravitational torques between the disk and planet, and their origin. In section 1, we outline the initial conditions for an additional series of simulations, not discussed in Paper I (the '*gap*' series of simulations), how we implement mass accretion in our code and the physical significance we can derive from it. We also summarize the main theoretical results for the derivations of gravitational torques between the planet and disk. In section 2, we look at accretion onto the planet, whether it can affect the migration rate, and given a lower limit on the accretion rate we discuss the likely morphology of the object. In section 3, we will examine in detail four simulations from Paper I (the low mass and high resolution prototypes with and without disk self gravity) in order to explore in quantitative detail the differences between our hydrodynamical simulations and linear analyses. Our purpose will be to determine the extent to which linear theory may be applied to the problem, as well as where and how it may fail. Lastly, in section 4, we compare our results to others in the literature.

1. The initial conditions and input physics

In this work we will make use of the 'low mass' and 'high resolution' prototypes, discussed in detail in Paper I . Briefly summarized, these models consists of a circumstellar disk with mass $M_{\rm D}$=$0.05M_{\odot}$, that extends from 0.5 to 20 AU. Mass is distributed according to an $r^{-3/2}$ power law and the temperature is defined by an $r^{-1/2}$ power law and the condition that the temperature at 1 AU is $T = 250$ K. We use an isothermal equation of state and the boundary conditions at the inner and outer edges of the grid are reflecting. For the low mass prototype, the disk is resolved on a 128×224 cylindrical[2] grid ($r \times \theta$), while for the high resolution prototype we doubled the grid resolution in each dimension, to 256×448.

The planet is set into an initially circular orbit at 5.2 AU and is thereafter influenced by gravitational forces from the $1M_{\odot}$ central star (fixed to the origin) and the disk. The gravitational softening required was

[1]UKAFF Fellow. Present address: School of Mathematics, University of Edinburgh, Edinburgh Scotland EH9 3JZ

[2]Throughout this paper and its companion, Paper I , we use 'θ' to denote the azimuth coordinate rather than the more usual variable 'ϕ' in order to avoid confusion between references to the coordinate and to components of the planet's gravitational potential, ϕ_m, common throughout this work.

defined to be equal to the size of the grid zone where the planet is found at each time. In order that the simulations would be identical, the high resolution prototype defined the softening to be twice the current cell size, so that the absolute values were identical. We have simulated two versions of these models, one with and the other without disk self gravity. All of our simulations studying accretion will include self gravity.

For our study of accretion we will use initial conditions and a physical model that are identical to our low mass prototype. We will perform two separate studies, one beginning from the low mass prototype, and the other with an already formed gap in the disk. We produce a gap from the unperturbed initial state by allowing the system to 'pre-evolve' for 3000 yr. In this pre-evolution, we begin with the low mass prototype, except that we assume that while the planet exerts gravitational forces on the disk, it is not in turn affected by the disk. Its orbit therefore remains fixed at 5.2 AU. During the pre-evolution, spiral patterns are generated by the planet/disk interaction and a gap structure forms in the disk. We show the unperturbed profile and the azimuth average of the mass distribution after 3000 yr in figure 1. While it is clear that the evolution has produced a significant change in the profile, the gap region is not totally devoid of matter. We monitored the profile during the evolution and found no significant changes during the last 1000 yr of this pre-evolution. We therefore believe that the system is at or near a steady state.

After the simulation has completed its pre-evolution, we save the resulting state 'as is' and use it as an initial condition for multiple simulations in which we 'turn on' the disk-on-planet gravity and allow the planet to migrate. One additional modification is required between the pre-evolution simulation and each of the models based on it. Turning on this additional gravity term requires that disk gravity be accounted for in the planet's velocity. We assume that the its orbit is circular and calculate the angular velocity required for its orbit from the net gravitational forces due to the disk and star.

1.1. The mechanics of accretion from a grid, and what we can learn from it

In the *acc* and *gap* series' of simulations (see definitions in section 2) we study mass accretion onto the forming planet. In these simulations, we allow mass to accrete onto the planet at a fraction, f, of the Bondi-Hoyle-Littleton (BHL) rate (**?**, see e.g.)]Shu2:

$$\dot{M}_{\rm pl} = 4\pi\rho_\infty f \frac{(GM_{\rm pl})^2}{(V^2+c_\infty^2)^{3/2}}. \tag{1}$$

We define c_∞ as the sound speed of the gas in the disk at the orbit radius of the planet and the velocity at infinity, V, is taken as the relative velocity of the gas with respect to the planet at the Hill radius, $R_{\rm H}$= $a_{\rm pl}(M_{\rm pl}/(3M_*))^{1/3}$, averaged over the azimuth region between the Lagrange points L4 and L5. The density at infinity is defined by an averaged surface density divided by twice the scale height, $\rho_\infty = \bar{\Sigma}/(2H)$. Guided by the results of Paper I , we determine the surface density average using the radial region between $a_{\rm pl}\pm 2R_{\rm H}$ and, as for the velocity, use the azimuthal region between the Lagrange points, L4 and L5.

At each time step an amount of mass $\dot{M}_{\rm pl}\delta t$ is added to the planet and removed from the disk region within one Hill radius of the planet. The mass removed from each grid zone is computed as

$$dM_{\rm zone} = -\dot{M}_{\rm pl}\delta t \left[2\left(1-\left(\frac{\mathcal{R}}{R_H}\right)^2\right)\right]\frac{r_i\delta r_i\delta\theta_j}{\mathcal{A}} \tag{2}$$

where $\mathcal{R}$ is the distance of the zone center from the planet, $r_i\delta r_i\delta\theta_j$ defines the area of a grid zone and surface area of the Hill sphere, $\mathcal{A}$, is taken as the sum over the areas of all grid zones for which $\mathcal{R}$ <$R_{\rm H}$.

We limit $dM_{\rm zone}$ to at most half of the mass in the zone, to avoid any potential instabilities caused by the sudden mass loss. With this definition, most of the mass removed is taken from the inner half of the Hill sphere nearest the planet, and no single zone suffers an unduly large change between successive time steps.

The accretion of mass onto the planet will of course be accompanied by some amount of angular momentum, both as an orbital component (around the star) and a spin component. We add this momentum to the planet and subtract it from each grid zone, so that the net result of the accretion conserves total angular momentum. The mass accreted onto the planet will change its orbital angular momentum both by increasing the planet's mass and by changing its trajectory. Mathematically, the change in orbital angular momentum of the planet due to accreting matter can be decomposed into three parts as

$$\frac{dJ_z}{dt} = \frac{dM_{\rm pl}}{dt} r V_\theta + M_{\rm pl} \frac{d}{dt}\left(r V_\theta\right) - \frac{dS_z}{dt}, \tag{3}$$

where r and V_θ are the planet's orbit radius and azimuthal velocity. The first term in this equation is due to the accretion of mass from the disk which is already co-moving with the planet. In other words, this change in angular momentum ('torque') has no net effect on the planet's trajectory. The second term represents the dynamical effect of the mass accretion and can be compared to the gravitational torques on the planet due to the generation of spiral density structures in the disk. We discuss the importance of this effect in section 2.1. The third term in equation 3 is necessary to properly account for the fact that the spin of the planet will also be changed by the accretion. This is because mass accreted onto the planet will in general not have zero angular momentum, as calculated around the center of mass of the planet and accreted mass.

While a Bondi-like accretion rate is not strictly valid for the geometry and flow pattern we consider here, we believe it represents an interesting limit. It is at or near the highest rate at which matter can be supplied to the planet by the disk and at or near the highest rate that the planet can accrete matter because it assumes that all matter within reach of the planet will be accreted and that none is able to build up into a long-lived envelope and oppose further infall. By including accretion or not we will be able to determine whether mass accreting onto the planet can bring with it enough orbital angular momentum (an effective torque), to significantly change the orbit of the planet. We will also be able to explore the conditions in the circumplanetary environment. Under what conditions is it reasonable to expect a circumplanetary disk to form? Should we expect the environment to be a somewhat spherical envelope, or something still more complex?

1.2. Analytic torque formulae

In section 3, we shall make detailed comparisons of the gravitational torques on the planet as produced in our simulations, to those predicted by theory. Here we will briefly state the torque formulae to which we make those comparisons. Analytic methods typically proceed by linearizing the equations of motion and evaluating the gravitational torques of the disk and planet on each other as the sum contributions from a Fourier series of density perturbations in the disk. The density perturbations are generated at an inner or outer Lindblad resonance (ILR or OLR, respectively) or a corotation resonance (CR).

?)][hereafter GT79, GT80]GT79,GT80 found that by far the largest portion of the torque exerted by a perturber is transmitted in the neighborhood of a resonance, and developed approximations for these torques that were based upon this fact. Because the torques are transmitted to and from the disk only at resonances, the torque on the planet can be expressed as the change in angular momentum flux through the disk at that resonance. Under this approximation, they found that the angular momentum flux generated by an m'th

order spiral pattern at Lindblad resonances is

$$F_{LR} = m\pi^2 f_c \left[\left| \frac{\Sigma(r)}{rdD/dr} \right| \left(r\frac{d\phi_m}{dr} + \frac{2\Omega}{\Omega - \Omega_{\rm pl}}\phi_m \right)^2 \right]_{r_L} \tag{4}$$

where D is the 'resonant denominator' and is defined as

$$D = \kappa^2 - m^2(\Omega - \Omega_{\rm pl})^2. \tag{5}$$

Ω and $\Omega_{\rm pl}$ are respectively, the orbit frequencies of each location in the disk and of the planet, and square of the epicyclic frequency is $\kappa^2 = 4\Omega^2 + 2r\Omega d\Omega/dr$.

The cutoff function, f_c, is introduced artificially to avoid numerically infinite torques for large m values. Its specific form is unclear, however Artymowicz (1993a,b) has given physical motivation for it in terms of the modification of the resonance locations due both to the pressure contribution to the rotation curve and to averaging the potential of the planet over the vertical thickness of the disk. He also derives an analytic approximation for it in the limit of an infinitely thin disk as

$$f_c = \frac{1}{H(1+4\xi^2)} \left[\frac{2HK_0(2H/3) + K_1(2H/3)}{2K_0(2/3) + K1(2/3)} \right]^2 \tag{6}$$

where K_0 and K_1 are Bessel functions, $H = \sqrt{1+\xi^2}$ and $\xi = m(c_s/r\Omega)_p$.

GT79 also approximate the flux due to interactions near corotation by

$$F_{CR} = \frac{-m\pi^2}{4}{\rm sgn}(x) \left[\left(\frac{\phi_m^2}{d\Omega/dr} \right) \frac{d}{dr} \left(\frac{\Sigma}{B} \right) \right]_{r_c} e^{-|qx|} \tag{7}$$

where $B = \kappa^2/4\Omega$ is the Oort parameter, $q = (r\kappa/c_s)_{r_c}$, $x = (r - r_c)/r_c$ and r_c is the corotation resonance location. In both equation 4 and 7, the gravitational potential of the planet, ϕ_m, is one term in an infinite series expansion in Laplace coefficients, $b^m_{1/2}$. In our comparisons, we calculate the Laplace coefficients using the method of Olvers (1967).

Equations 4 and 7 have been further refined by, e.g. Ward (1988); Artymowicz (1993a); Ward (1997) and Takeuchi *et al.* (1996). In particular for the LRs, the inclusion of non-WKB terms in the wave equation, and will result in a modified resonant denominator

$$D_* = D + \left(\frac{mc_s}{r} \right)^2, \tag{8}$$

which modifies the effective resonance positions for higher order m patterns by creating a buffer region around the planet, where the resonances would normally fall. A similar quantity that accounts for disk self gravity (Artymowicz 2001, personal communication) is

$$D_{sg} = D + \left(\frac{mc_s}{r} \right)^2 - 2\pi G\Sigma \left(\frac{m}{r} \right). \tag{9}$$

In some analyses, the Laplace coefficients in the potentials are approximated by Bessel functions,

$$b^m_{1/2}(\alpha) \approx \frac{2}{\pi} K_0(m|1-\alpha|) \tag{10}$$

where $\alpha = r/a_{\rm pl}$, $a_{\rm pl}$ is the semi-major axis of the planet and r is evaluated at the Lindblad resonances. For an exactly Keplerian rotation curve, the argument of the Bessel function is nearly constant (at 2/3) for all

m patterns at all Lindblad resonances. Both Ward (1988) and Korycansky & Pollack (1993) have defined a generalized Laplace coefficient in very similar ways in order to avoid numerical singularities at the planet's orbit radius. Using the form from Korycansky & Pollack (1993), it is

$$b^m_{1/2}(\alpha) = \frac{2}{\pi} \int \frac{\cos m\theta d\theta}{\left(s^2 + p^2\alpha^2 - 2\alpha\cos m\theta\right)^{1/2}}. \tag{11}$$

where $p = 1$, $s = 1 + r_0^2/a_{\rm pl}^2$ and r_0 is the softening radius. The interpretation given to this modification is to account in an approximate way for either a numerically required softening coefficient (Korycansky & Pollack 1993) or (in a slightly different form) the vertical structure of the disk (Ward 1988). In combination, the improvements of the theory represented in equations 8, 9 and 11 are sufficient to negate the need for the cutoff function. In general, we will use only this form (without the cutoff function) in our comparison calculations but will also make comparisons to the form defined in equation 10 in order to investigate the changes in the torques they are responsible for.

Using these analyses, the torque of the disk on the planet will be the amount of flux injected into or removed from the disk at a given resonance. For the Lindblad resonances, wave propagation is forbidden between the ILR and OLR and the flux is zero there. Therefore, we can calculate the theoretical torque on the planet if we calculate the angular momentum flux at the resonance, using equation 4. For the corotation resonances, the torque on the planet may be calculated from equation 7 as the difference between the left and right limits as r approaches r_c.

The torque, δT, exerted on any given ring, δr, in the disk is accounted for as a torque density, dT/dr, as is the torque actually transmitted to the disk matter. The first form will be a function of the amplitude and phase of a wave as it propagates through the disk and in the second will be a function of the dissipation in the disk as it decays. In the first case, studied by Ward (1986), the torque density will be characterized by an oscillating function of distance from the planet while in the second (Takeuchi *et al.* 1996), the torque will instead be a decaying function of distance. Since our interest lies mainly in the torque of the spiral pattern on the planet, our torque densities will be characterized by the oscillatory form. Corotation torques on the other hand are not associated with waves. Torque densities on the disk for these resonances may be obtained directly from equation 7 by differentiation with respect to r.

1.3. Deriving torques from the simulations

In order to make comparisons to the torque formulae above, we must determine the amplitude and phase of each Fourier component of spiral density structures present in our simulations. As a function of radius, these amplitudes are

$$X_m(r) = \frac{1}{\pi} \int_0^{2\pi} e^{im\theta} X(r,\theta) d\theta, \tag{12}$$

where X is the perturbed quantity (in this case surface density) and $m > 0$. With a normalization of $1/2\pi$ for the $m = 0$ pattern, the sum over all m components yields the surface density at radius, r, and azimuth angle, θ. In our discussions below we will normalize the surface density amplitudes for all patterns to the Σ_0 (i.e. azimuth averaged) component. The phase of each component is

$$\theta_m = \tan^{-1}\left[\frac{Im(X_m)}{Re(X_m)}\right]. \tag{13}$$

Calculation of the torque on the planet is a straightforward reconstruction of the density due to each pattern in each grid zone and a sum of the net torque over all grid zones. With a change of sign, these torques are also those exerted by the planet on the gas in the disk at each radius, and the summation can be separated into two partial sums to account for torques from radially inward or outward of the planet.

1.4. Connection of the numerical results to physical systems

In following discussion, we will show the torque magnitudes and torque densities exerted by the disk on the planet, either due to accretion or to gravitational interactions. As a point of reference in evaluating the figures, recall that the present day Jupiter has a total orbital angular momentum of 1.9×10^{50} g cm^2/s. Therefore a torque of 10^{38} g cm^2/s^2 exerted for a time of 10^3 years will cause it to migrate inward from 5.2 AU to 5.0 AU. A $0.3M_{\rm J}$ planet would move inward to 4.6 AU under the same influence. When spread over a radial region of 0.25 AU, a torque of this magnitude yields a torque density of $\delta T/\delta r \sim 7 \times 10^{24}$ g cm/s^2.

2. The importance of accretion on planet migration

Many workers have shown in linear and nonlinear analyses that a planet embedded in a disk, especially before a gap has formed, is expected to have strong dynamical interactions with the disk matter within a few disk scale heights radially inward and outward of the planet. We found in Paper I that in fact the migration was dynamically very sensitive to the disk mass close to the planets-within one or a few Hill radii in both radius and azimuth coordinates. One additional interaction specific only to this region is mass accretion. In the following sections, we examine the importance of mass and momentum accretion onto the planet on its trajectory and the formation of a gap using simulations that allow accretion onto the planet at varying rates. We then inquire into the physical reasonability of those rates, in order to better constrain the possible morphology and growth processes of forming planets. The parameters defining each of the simulations in these experiments are summarized in table 1.

2.1. Accretion

We saw in Paper I that planets with enough mass can open a deep gap in the disk via gravitational torque interactions and in so doing drastically slow their migration. Since the disk begins in a somewhat artificial condition (a $1M_{\rm J}$ planet should have already either formed a gap or been accreted by the star) we cannot consider the rapid motion prior to gap formation typical behavior of the long term behavior of real systems with such massive planets.

Lower mass planets remain at issue. The migration of a planet less massive than $0.3M_{\rm J}$ does not lead to a gap and is fast enough to move inward on a $<< 10^5$ yr time scale, far shorter than the expected disk lifetime of $> 10^6$ yr and the expected formation time scale for planets. The critical conclusion to note is that low mass planets can be influenced by gravitational torques from the disk strongly enough to migrate quickly through it, but cannot influence the disk strongly enough to form a deep gap and enter the much slower Type II migration phase. How then can such objects survive long enough to remain separate from the central star as the system moves into its main sequence lifetime?

Accreted matter changes the angular momentum of the planet due both to the increase of mass and because that matter does not in general have identical specific angular momentum to the planet when it is accreted. Additional matter accreting onto the planet continues to bring with it orbital angular momentum, exerting an effective torque on the planet's trajectory. If forming planets are to survive for more than a few thousand years, then at least one of three conditions about this accreted matter must be true. First, if this angular momentum contribution is positive (and large enough), then it will provide a positive torque on the planet, counteracting the negative dynamical torques acting on it. Second, the planet could accrete all of the nearby disk matter, thus opening a gap and eliminating the large gravitational torques driving the migration. Third, mass accretion onto the planet could proceed faster than Type I migration, so that planets become massive enough, quickly enough to transition to Type II migration before migrating all the way inward to the stellar surface. Each of these possibilities can be true only if the disk can supply matter at a fast enough rate and the planet can accept matter at that rate.

We have explored the viability of these three conditions with a set of simulations that include accretion onto the planet, and use our low mass prototype simulation as a model. In order to test whether the evolution is merely an artifact of the fact that our initial condition is an unperturbed disk, we consider two cases. We consider an initial condition identical to our low mass prototype, and we consider an initial condition which begins with an already formed gap in the initial surface density profile around the planet, as shown in figure 1. These two series are designated *acc* and *gap* in table 1, respectively. For each series, we vary the accretion rate by changing the assumed fraction, f, of the Bondi-Hoyle-Littleton rate (see eq. 1) in different simulations.

Is the accretion torque positive and large, satisfying our first condition? In figures 2 and 3, for the unperturbed and initial gap simulations respectively, we show the accretion torque as a function of time for a high accretion rate and for a low accretion rate simulation. For the two $f = 1$ models, the torque magnitude is initially large compared to the dynamical torques exerted on the planet by individual spiral patterns (see section 3.1 below), but within $\lesssim 500$ yr drops to near zero as the planet accretes additional mass. In both examples, the migration of the planet proceeds inward from 5.2 AU to 4.8 AU and stops. The low accretion rate models each have accretion torques which are far smaller than the dynamical torques on the planet. In the *acc4* model, the migration proceeds in near identical fashion to the low mass prototype simulation, while the *gap4* model, the planet remains at 5.2 AU for the duration of the simulation. The sign of the torque is always negative. Therefore it acts to increase the planet's inward migration rate, and we conclude that a planet's migration cannot be halted by the accretion of orbital angular momentum from the disk. Our first condition is not confirmed.

Can a forming planet can accrete all of the nearby disk, thus forming a gap and satisfying our second condition? In figure 4, we show the mass of the forming planet as a function of time for different fractions, f. For fractions, $f \geq 0.01$, the planet accretes between four and eight $M_{\rm J}$ of mass from the disk in only 1800 yr. The initial accretion rates are as high as $\sim 1 M_{\rm J}/25$ yr in the most extreme cases. The accretion occurs so quickly that the limiting factor in the accretion is not the BHL rate given by eq. 1, but rather the fact that the disk simply cannot supply matter to the planet at the calculated BHL rate fraction. Instead, the rate is limited by the maximum amount of mass that we allow to be removed from a given zone per time step. The region inside the Hill sphere of the planet becomes completely drained and a gap is quickly generated in the disk as matter continues to pass into the planet's Hill sphere. As found by Bryden *et al.* (1999) and Lubow, Siebert & Artymowicz (1999), we also find (by virtue of the fact that this region is the first to be emptied of matter) that matter accretes onto the planet first from the regions approximately 2-4$R_{\rm H}$ inside and outside the planet's orbit radius. Matter in the 'horseshoe' region, at the planet's orbit radius but with

a phase relative to the planet greater than $\pm\pi/3$, is able to remain unaccreted for longer periods, but is also lost within 10^3 yr when $f > 0.01$.

The accretion rate decreases only when a wide and deep enough gap has begun to form in the disk. When such a gap begins to form, a relatively smaller amount of matter can come into close contact with the planet, and so become perturbed onto a planet intersecting orbit and accreted. The planet masses at which this turnoff occurs in the *gap* simulations are a factor of ~ 2 below those reached in the *acc* series. While it is true that the 'final' masses for the planet at the end of each simulation are smaller by about a factor of two, the basic conclusion remains. These rates are sufficient to increase the planet's mass to several Jupiter masses in only a few hundred years.

For a $0.05M_\odot$ disk, more than $20M_{\rm J}$ are available to be accreted in the region $\pm$ 1 AU from the planet, so that the planet would reach a mass of several tens of Jupiter masses rather than the $\sim 6-8M_{\rm J}$ that it reaches before the accretion slows. This means that the disk does not supply matter to the planet at a rate such that *all* of the nearby disk matter is accreted. Therefore our second condition is not confirmed. However, planets this massive still do open a gap and make the transition to Type II migration via dynamical processes alone, as we saw in Paper I . This means that the disk is capable of supplying the planet with matter quickly enough to drive gap formation by dynamical processes, so that our third possibility may be confirmed if the planet can accept matter at these rates.

Our first two conditions for survivability of Jovian planets (torques due to accretion and accretion of all available matter) could be definitely ruled out in this section. While accretion of additional mass can indirectly drive gap formation by dynamical processes, the accretion torques have little direct effect on halting or accelerating the migration, even for the most extreme simulations we performed. These conclusions are true for both the unperturbed and initial gap simulations and so are not an artifact of the initial condition. The third condition (accretion of enough matter to open a gap via dynamical processes) could not be confirmed or ruled out directly. However, we can take the information that Jovian mass planets exist around the sun and other stars, along with the failure of our first two possibilities, as an indirect confirmation. One significant ambiguity remains however: how fast can mass accretion onto the planet actually proceed?

2.2. The morphology of the circumplanetary environment and its influence on the planet's accretion rate and final mass

Deriving limits on the planet's accretion rate is important for both the survivability of the planet and determination of its final mass. In this section, we will set a lower limit on the accretion rate from the condition that it survive long enough to form a gap, and a (weak) upper limit by examining the morphology of the planet implied by the accretion. We will conclude that the planet's envelope must undergo periodic dynamical instabilities during this phase of its evolution. The efficiency of these instabilities in accelerating the mass accretion will influence the final mass of the planet.

We can define a lower limit on the mass accretion rate of the forming planet from the results Paper I . We know that low mass planets migrate on a time scale of order 0.5–1 AU per thousand years, and can open a gap when they reach $\sim 0.3M_{\rm J}$. This means that in order to survive long enough to open a gap and slow their migration rate, planets less massive than $0.3M_{\rm J}$ must grow faster than $\sim 10^{-4}M_{\rm J}$/yr. The limit will be somewhat lower in disks less massive than the $M_{\rm D}/M_*$=0.05 ratio implicit in these calculations, but recall that we are considering a relatively early stage in the planet's evolution when the disk may still be more massive than the nominal minimum mass solar nebula.

How much larger than this lower limit can the accretion rate be? The efficiency of accretion will depend to some extent on the distribution and dynamic and thermodynamic conditions of mass very close to the planet. For the planet masses discussed in our study, any envelope that existed earlier has grown massive enough that gravitational contraction and/or ejection of some of the matter has begun (Bodenheimer & Pollack 1986; Wuchterl 1991). Eventually the forming planet will begin to develop a central core+disk structure. If we assume a disk structure has already formed, we can derive a self-consistency check of this assumption from the gravitational potential energy that must be radiated by the gas before it is accreted onto the planet and from a measure of the disk's thickness.

For a given accretion rate, and independent of the specific form of dissipation in the disk, the central temperature for a steady state, internally heated accretion disk is given by

$$T(r) = \left(\frac{9GM_{\rm pl}\dot{M}_{\rm pl}\tau}{32\pi\sigma} \right)^{1/4} r^{-3/4} \tag{14}$$

where τ is the optical depth to the midplane and σ is the Stefan-Boltzmann constant (**?**)ch. 5]FKR. This formula is general in the sense that it assumes only that the disk is optically thick and that the accretion rate is constant.

A dimensionless measure of the scale height is $H/r = c_s/(r\Omega)$. If we assume that $H/r = 1$ (a serious violation of the thin disk criterion), then we can convert the scale height into a temperature

$$T(r) = \left(\frac{\mu m_{\rm pr} G M_{pl}}{\gamma k_B} \right) r^{-1} \tag{15}$$

where $m_{\rm pr}$ is the mass of the proton, k_B is Boltzmann's constant, μ is the average molecular weight of the gas and γ is the ratio of specific heats. In order for the circumplanetary environment to be 'disky', gas temperatures must be well below the limits defined by eq. 15.

For what accretion rates are such temperatures obtained in the circumplanetary environment? In order to answer this question we require the values of the average molecular weight and the ratio of specific heats which, for conditions appropriate for circumplanetary disks, will be $\mu \approx 2.3$ and $\gamma \approx 1.4$. We also require a value for the optical depth, $\tau(= \Sigma\kappa)$. We can make a very conservative estimate of the surface density, Σ, if we assume that the circumplanetary disk mass at given time is the mass of the present day Jovian moon system, which we will assume at the time of formation to consist of both gas and solids in solar nebula proportions. Then the surface density is $\Sigma \sim 10 - 20$ g/cm^2 for a disk extending outwards to the Hill radius. For a solar composition, the Rosseland opacity of this matter at typical nebular temperatures will be $\kappa \sim 2 - 4$cm^2/g (Pollack *et al.* 1994), so that the optical depth is $\tau = \Sigma\kappa \sim 10 - 100$.

For an optical depth of $\tau = 100$, equations 14 and 15 yield curves as plotted in figure 5 for a $0.3M_{\rm J}$ planet. The condition that the disk have $H/R = 1$ is defined by a temperature of $T \approx 200$ K at a distance of one Hill radius (0.24 AU) from the planet and reaches the destruction temperature of silicate dust ($T \approx 1200$K) at a distance of 0.04 AU from the planet ($\sim 40 - 50R_{\rm pl}$ if $R_{\rm pl}$=$2R_{\rm J}$). For all accretion rates $\dot{M}_{\rm pl} > 10^{-4}M_{\rm J}$/yr, the condition that the disk be thin is severely violated in all but the innermost parts of the circumplanetary disk. Lower mass planets will have curves with similar characteristics, but with lower temperature scales, through the ${M_{\rm pl}}^{1/4}$ and ${M_{\rm pl}}^{1}$ proportionalities in the temperature laws, eq. 14 and 15, respectively.

Coupling this result to the lower limit on the accretion rate, we conclude that survival of the planet is inconsistent with the assumption of a circumplanetary disk at this stage of the planet's evolution. For most of the time that it is growing, the planet must accrete matter faster than $\dot{M}_{\rm pl} > 10^{-4}M_{\rm J}$/yr. This conclusion

places a strong constraint on the planet's morphology. It must be characterized by an envelope or thick disk structure.

We can use this constraint to derive a weak upper limit to the accretion rate. The most liberal upper limit is that at which radiation pressure suppresses accretion of additional material. Assuming that the opacity source is ionized hydrogen atoms, then this rate is the Eddington accretion rate, which for an accreting surface at a radius $\sim 1 - 2R_{\rm J}$, is $\sim 10^{-1} M_{\rm J}$/yr. However, the Eddington rate is probably not relevant for accreting Jovian planets in circumstellar disks, because the main source of opacity is not ionized hydrogen, but rather dust or exited states of complex molecules. If we instead assume that the main opacity source is dust and that the gas and dust remain well mixed, then the appropriate mass opacity is the $\kappa \sim 2 - 4 {\rm g/cm}^2$ value noted above rather than the $\kappa \sim 0.4 {\rm g/cm}^2$ appropriate for Eddington accretion, and an analogue of the Eddington rate would be a factor ten smaller.

A much more restrictive limit than radiation pressure is the requirement to overcome the gas pressure of the planetary envelope composed of the recently accreted matter. This rate is available from an analysis of the Kelvin Helmholtz contraction of the envelope. Bryden *et al.* (2000) define the maximum accretion rate allowed by Kelvin-Helmholtz contraction of the envelope as

$$\dot{M}_{\rm KH} = M_{\rm KH0} \left(\frac{M_{\rm pl}}{M_\oplus} \right)^4 \tag{16}$$

where $M_{\rm KH0} = 7 \times 10^{-11} M_\oplus$/yr. For a planet with mass $0.3 M_{\rm J}$, we derive an accretion rate of $\sim 6 \times 10^{-3} M_\oplus$/yr, or $\sim 2 \times 10^{-5} M_{\rm J}$/yr. For a planet of half as massive, the rate is $\sim 10^{-6} M_{\rm J}$/yr. Although Bryden *et al.* (2000) discuss a number of factors that can affect this accretion rate, none are likely to change it by the factor 100 or more required to grow faster than the migration. Therefore we have an *upper* limit for mass accretion which is substantially lower than our *lower* limit.

Even ignoring the Kelvin-Helmholtz contraction, the upper limits from radiation pressure alone are already smaller than the accretion rates obtained for our models with accretion factors $f = 1.0$ and 0.1, eliminating them from the parameter space of systems with physically self-consistent evolution. Elimination of these models is significant because we can conclude that the accretion rate onto forming Jovian planets is driven primarily by conditions near the planet, and not by conditions in the disk. The gas accretion phase of planet formation, in which the planet accretes the largest fraction of its final mass, is therefore relatively insensitive to the disk mass except insofar as it sets the migration rate through the disk. This conclusion has rather far reaching consequences because it is in essence a statement that Jovian planet formation and the initial mass function for Jovian planets are sensitive to the small scale physics in the forming body–physics such as the planetary spin and opacity (metallicity) which are common to all such systems–and much less sensitive to the global thermodynamic or physical properties of the star+disk system.

The rates derived from radiation and gas pressure both define upper limits to the accretion rate onto the planet. We characterize these limits as 'weak' because they are dependent on assumptions that are probably not met in practice. One assumption that is particularly dubious is the neglect of the planet's spin and spin accretion rate in our estimates. We find that many times Jupiter's present spin angular momentum is accreted during the 1800 yr of evolution followed in our simulations. Undoubtedly this value is inaccurate–due both to our low resolution and to our neglect of angular momentum exchange between the planet and disk, but it serves to draw attention to one point. If rotation plays an important dynamical role in the growth, then dynamical instabilities may develop in which the envelope becomes unstable to spiral structure growth and rapid mass transport.

In one dimensional calculations, Korycansky *et al.* (1991) showed that when exchange between the

envelope and circumstellar disk is allowed, only $\sim 2-3\%$ of the angular momentum remained in the planetary system, with the rest immediately returned to the solar nebula. Since their calculations were one dimensional, they could make no statements about the nature or mechanism for this transport however. Rotational instabilities are known to develop in morphologically similar entities such as rotating polytropes (Pickett *et al.* 1996; Toman *et al.* 1998). We speculate that the mass accretion rate in forming Jovian planets could be enhanced if large scale dynamical instabilities in the planet's envelope could develop, due to this spin accretion and the processes that return it to the solar nebula. Clearly, much more work is required before a more firm conclusion can be drawn on this point.

3. The dynamical interaction of the planet and disk

In Paper I and in section 2 we studied the planet and the disk somewhat qualitatively in terms of their actions on each other and the consequences for the evolution. We found that some of the major qualitative predictions of analytic theories were only partially recovered in our simulations. Here, we will attempt to make the analysis more quantitative in terms of the applicability of analytic formalisms to the system, and in what limits they break down. Because of the large and important differences in outcome, depending both on grid resolution and on whether disk self gravity was included or not, we will do a side by side analysis of four models from Paper I : the low mass (with our 'standard' resolution of 128×224) and high resolution prototype models with and without disk self gravity. The standard resolution (in the low mass prototype) vs. high resolution comparisons will provide insight into the role of the mass distribution in the torque calculations, while the self gravitating vs. non self gravitating models provide insight into the physical model itself. In a sense, these comparisons will also touch on the differences between gap forming and non gap forming systems, since the two models with self gravity form gaps, while those without it do not.

In sections 3.1 and 3.2, we show the torques from our simulations, first as a function of radius, then as a function of Fourier pattern number, m, and compare them to the analytic predictions. Then in section 3.3 we examine the approximations made in deriving the analytic torque formulae and the approximations made in our numerical realization of the system. While very important for mathematical models of migration, this discussion will be rather detailed and of lesser interest to some of our audience. These readers may safely skip forward to section 3.4, where we discuss the consequences of failures of various mathematical assumptions on the gravitational torques when they break down.

3.1. The torques exerted by the planet and disk on each other

In figure 6, we show plots of the gravitational torque density of the disk on the planet as a function of radius for the low mass and high resolution prototype simulations. The torques densities shown are those at the same time (300 yr), as in the top panels of figures 4 and 6 of Paper I , for which spiral patterns have fully developed and have had time to propagate through the entire disk, but before a deep gap has formed. These torques will be representative of those expected from Type I migration assumptions.

In each case, the torque density is very large near the planet (radially) and decays as a function of distance inwards and outwards from the planet, as the spiral patterns themselves decay. Qualitatively, the morphology present is consistent with the theoretical model that low order m patterns contribute little to the total torque, and that higher order m patterns, whose resonances fall closer to the planet, are excited and provide most of the net torque contribution. The sign of the torque oscillates so that at some radii it acts

to increase the disk's angular momentum at the expense of the planet, while at other very nearby locations it acts in the opposite sense. The oscillations are stable in time relative to the planet's position. The torque curves shown with the dotted line (omitting the contribution from inside the Hill sphere) shows that while the matter inside the Hill sphere makes some contribution to the total, it is not by itself the determining contribution to the torque from this radial region.

The contribution to the total due to the $m = 1, 2$ and 10 spiral patterns are shown in figures 7 and 8, for the same four models. In each case, a torque oscillating in sign originates at an LR and extends with decreasing amplitude in the direction away from the planet. Consistent with our resolution dependent numerical dissipation, the lowest order (longest wavelength) patterns propagate the furthest distances from the planet and produce torques over nearly the entire radial extent of the disk, while higher order patterns contribute to the torques only very close to the planet. The low order m patterns each display a large torque near the planet as well, clearly distinct from the oscillating torque pattern further away and presumably due to the corotation interaction.

The $m = 1$ pattern represents a special case pattern–it has no inner Lindblad resonance. Therefore we expect that no spiral structures should be generated there and no torque on the planet from interior to its orbit due to this pattern should exist. Indeed this is the case–the torques from the $m = 1$ pattern from well inside the planets orbit are near zero, while a decaying wave structure in the exterior disk is visible. The $m \geq 2$ patterns do have both inner and outer Lindblad resonances and for the $m = 2$ pattern, the torque oscillates in sign and decays as a function of distance from the planet, while for the higher order symmetry $m = 10$ pattern only the first wave maximum can be observed.

In each case, the torques and their oscillations are larger in the non self gravitating disks than in the self gravitating versions. This is most likely a consequence of the difference in the migration rates and their effect on the forming gap. Although we have attempted to examine a point in time before substantial evolution has occurred, gap formation has begun to reduce the surface density near the planet, unfortunately causing the torques to be decreased by varying amounts in each simulation. While slightly visually disturbing, the differences will have few if any consequences for our comparisons below.

Each pattern also produces a large torque contribution from locations radially very close to the planet, near the corotation resonance locations and where waves generated from Lindblad resonances are forbidden. For all simulations except the high resolution non self gravitating version, the contribution is positive in sign (increasing the planet's angular momentum) both inside and outside the planet's orbit, but negative in sign (decreasing its angular momentum), slightly further inward. These torques are resolved on our grid in the sense that they are distributed over many radial rings of grid zones, however they differ greatly in character between simulations at different resolution. Therefore, we believe that their true character is not fully resolved by our simulations.

3.2. Comparison to linear analyses

We have seen above that the torques on the planet can include some contribution from locations far from resonance locations, and torques from near both the corotation and Lindblad resonances. Cursory examination of figures 6–8 suggest that some characteristics predicted by theory for those resonances may not be identically reproduced in the simulations (e.g. we would expect from equation 7 that the torque near CR would have the same sign over the entire radial range where it is exerted, but this is rarely the case). Nevertheless, we will proceed by identifying the torques from the region around each resonance location,

with the interaction predicted theoretically for that resonance. Separating these torques from each other in our simulations however, proves to be a challenging problem because for higher order m patterns, the Lindblad resonances are found progressively closer to the planet.

For the lowest m patterns, a clear separation exists between the CR and LR torques because their positions are well separated from each other. Therefore, for the purposes of our study, we shall define the LR torques as those exerted in the region between $r = \infty$ ($r = 0$) and the point half the distance between the Lindblad resonance and the corotation resonance for the OLR and ILR torques respectively. This allows us to include the portion of the torque which may be produced at some distance from the resonance itself, but nevertheless is clearly associated with it. We arbitrarily assign the difference between the total torque and the sum of the two LR contributions to the corotation resonance. For higher m patterns (above $m = 15$), where all three resonance locations are very close together and it becomes impossible to distinguish between the torques from the LRs from the corotation torque, we shall assign the entire torque to the LRs.

3.2.1. Torques from near the Lindblad Resonances

The contributions to the torque from each Fourier component and due to the Lindblad resonances are shown[3] in figure 9 and 10 for the models with and without disk self gravity. We also show the torques broken down to show the contribution from inside and outside the planet's orbit. Differences exist, but in general, many qualitative features obtained for the different runs are similar to each other. In each simulation, the dominant contribution to the torques comes from the spiral patterns with $10 < m < 20$ and as m increases, the torque magnitude contributions decrease monotonically to zero. Below $m = 20$, the total LR torque may change by a factor of two or more between one pattern and its neighbors of higher or lower symmetry. For most patterns, the total Lindblad torque is negative, but this is not universally the case. In each of the simulations for example, positive total torques are present for the patterns near $m \sim 5$.

While the inner (positive) torques are quite similar to each other in all four simulations, the outer (negative) torques are larger in the non self gravitating disks than in the self gravitating versions, especially for the higher m patterns. This is consistent with the result that planet migration proceeds more rapidly in absence of disk self gravity. In the high resolution versions, there is more variation between the torques of individual patterns, probably because of the improved ability to distinguish them from the CR torques.

Also shown in figures 9 and 10 are the torques predicted from equation 4. To derive these torques, we use the azimuth averaged surface density and rotation curves of each simulation as inputs and include the generalized resonant denominator of equations 8 or 9 both to determine the resonance positions and in the torque formula itself. We also use the generalized Laplace coefficients of equation 11, with the same softening as is used in the simulations. Some qualitative features are reproduced well by the theoretical calculations. In each case, the torques are small for both small and large m, with maxima in both the net and inner and outer torque contributions near $m = 10$. The positive net torques near $m \sim 5$ are also reproduced.

There are also several very serious differences between the torques from theory and from simulation. The most significant is that in each case, the torques from theory are systematically larger by as much as a factor of six, than those from the simulations. Secondly, the torques in the non-self gravitating versions are larger than those in the corresponding self gravitating version. In three of four simulations, the torque distributions

[3]Here and throughout, we shall plot the torques as continuous functions of the (integer valued) Fourier pattern number m, rather than plotting their values as points, in order to enhance readability of the plots.

from theory are smoother as functions of m in the sense that variations between nearby m patterns are small. The exception is the high resolution self gravitating model, which produces a large, negative net torque at $m = 8$ and a large increase in both the inner and outer torques near $m = 10$, gradually decreasing as m increases.

3.2.2. Torques from near the Corotation Resonances

Figure 11 shows the total torques on the planet from the corotation resonances with $m \leq 15$. In each simulation, the most striking feature is that many patterns produce torques that are as large or larger than the net contribution from the LRs. The contributions for the patterns with $m \lesssim 3$ are particularly interesting because not only are they large, they are also positive, thus acting to slow the inward migration of the planet. For patterns with $m > 3$, the torques are negative and again significant in magnitude compared to the torques from the LRs. Only for patterns with $m > 10$, do the torques decrease to near zero and only when disk self gravity is present. The net torque from the CRs with $m \leq 15$ is about a third the value of the torque from the LRs.

After the simple observation that many of the CR torque components are large, we are confronted with the uncomfortable situation that large differences that exist between the results of each of the simulations, including differences between the simulations which differ only in resolution. The most significant differences are found in the magnitude of the torque from the $m = 1$ pattern. It is larger when self gravity is not included and it increases by nearly a factor of two when we increase from our standard to high resolution.

In both the standard and high resolution versions without self gravity, the torque from $m = 1$ was so much larger that it could not be displayed on the plot while also displaying features from $m > 1$. The same was true in figure 8 for the radial distribution of the torque. More important to note than its exact value is that the contribution is more than three times the largest one sided LR torque (i.e. ILR or OLR). It also has no counterbalancing torque of opposite sign as the LRs do, making its contribution very important in a determination of the migration rate. Further, for the high resolution simulations (but not the standard resolution models), the torque is large and positive when disk self gravity is included, but large and negative when it is suppressed.

Higher order m patterns also display differences. While the standard resolution simulations have near zero CR torques, both of the high resolution counterparts have large negative torques. In this case, both high resolution simulations produce negative torques for $5 < m < 10$, so that the inward migration is more rapid. Above $m = 10$, only the non-self gravitating simulation produces negative torques.

Because of the large and qualitative differences between the simulations, we are forced to conclude that we have not adequately resolved the effect that the CR torques will have. We have therefore not attempted to make a direct comparison of the CR torques with their analytic predictions, as we have for the LRs. While we cannot make reasonable comparisons with theory, we may still draw important physical conclusions from the large size of the CR torques. Namely, that they may have a much larger effect on migration than previously realized. In order to constrain this possibility further, extremely high resolution global simulations of disks during the Type I migration stage must be performed.

3.3. Examination of the Assumptions and Approximations Made in Linear Analyses

What is the origin of the serious differences between theory and simulation, and between one simulation and another? In this section, we will examine the effects of the variation of the rotation curve on the torque and small shifts in the resonance locations may have on the calculated torques, and in the following section, their significance for the torques. Such shifts may be global in nature, for example a shift in the initial state due to self gravity or pressure forces. Variation in the rotation curve may also be more local in nature, for example the changes in the rotation curve due to steep pressure gradients at the edges of the forming gap. Except for the discussion of linearity in section 3.3.2, in the following sections we will concentrate specifically on our high resolution prototype simulation (with and without self gravity) so that these small shifts may be determined more precisely.

3.3.1. Validity of the resonance approximation

The wavelike behavior of the lowest order patterns is a consequence of the fact that at some radii, the spiral patterns have a different phase relative to the planet than at other radii. The torque exerted on the planet by the disk matter at that radius is therefore positive or negative depending on this phase. The important points to note are that the torque is exerted at locations significantly different from the Lindblad resonance and that the sign of this local torque can be opposite that of the prevailing flow of angular momentum.

How much do the torques exerted far from the resonances contribute to the total? This question is important because one simplifying assumption made in deriving equations 4 and 7 is that the disk and planet interact only *at* the resonances, rather than at some distance away from it. Errors in the comparison will enter if torques far from resonances contribute a significant fraction of the total.

Based on inspection of figures 7 and 8, the simulation most strongly affected by torques far from the resonance will be the non self gravitating, high resolution version because its torques have the largest amplitude oscillations everywhere. For this model, figure 12 shows show the cumulative sum of the torque as a function of distance from the planet (both inward and outward) originating from the Lindblad resonances, Torques from corotation interactions are suppressed. While some errors are made due to incorrect separation of the CR and LR contributions, in every case the cumulative torque magnitude increases to its maximum value slightly outside or inside the exact resonance position for the OLR or ILR respectively. At greater distances, it undergoes decreasing amplitude oscillations around what becomes its final value at large distances from the planet. In every case the oscillations are smaller in amplitude than in the first 1/2 cycle of the wave. Therefore, the largest fraction of the net torque from a given resonance is indeed derived from near the resonance position itself.

The maximum cumulative torque is never obtained at the resonance, but rather slightly further away from the planet, after which the cumulative sum falls to a value as much as 30–50% below its initial maximum. This is to be expected since the torque density waveform can be approximated as an Airy function (Ward 1986) whose first maximum is found about 1/4 cycle more distant from the planet than the resonance. The correspondence is also strengthened by the fact that the integral (i.e cumulative sum) of the Airy function also drops nearly 40% from its initial maximum during the next 1/2 cycle of the wave.

A useful visual diagnostic for comparison between patterns is the position of the first maximum of the cumulative torque relative to the resonance position. Using this measure, there is variation between one

pattern and another. For the $m = 2$ pattern for example, the ILR position is at approximately the half maximum, while the OLR position, even accounting for the positive offset from misattributing a portion of the CR torque to the LR, is found nearly at the 'foot' of the wave. Variation similar to that shown are present in all other patterns as well.

We conclude that the resonance approximation of GT79 is partially supported by our simulations for at least the Lindblad resonances, since most of the torque between the planet and the disk originates from the first cycle of the wave. Our method of separating the CR and LR torques already constrains the CR torques to a narrow region, so we can make no statements about these contributions. The specific approximation that the conditions at the *exact* resonance position can be used to determine the torque may not be as well justified, because the maximum cumulative sum may be found at varying distances from the exact resonance.

3.3.2. Linearity

In Paper I we found that the migration rates were nearly flat as a function of planet mass, varying by less than a factor of two over a factor 20 change in mass. In contrast, theory predicts that the rates will scale linearly with planet mass. The theory is based on the assumption that the perturbations are small, so that the models are in the linear regime. In this limit, we expect the perturbations to scale with the mass of the perturber, and through them also the migration rate. If instead perturbations are large, they will saturate–larger perturbers will not produce larger perturbations.

Are our migration rates flat because the perturbation amplitudes are saturated? In figure 13, we show the maximum pattern amplitudes as a function of mass (i.e. for the *mas* series of simulations–see Paper I), obtained in the regions defined for each of the three resonances, each obtained at a time 300 yr after the beginning of the run. We again show the $m = 1, 2$ and 10 patterns as typical representatives of the behavior of each of the other low and high order symmetry patterns.

The $m = 1$ and $m = 2$ pattern amplitudes may reach as high as 40–50%. Even with these very large amplitudes, a close correlation between the relative amplitudes of each of the three resonances with each other is maintained. Although we have not attempted to fit linear functions to the data, a clear linear increase is present over most of the mass range. For example, the amplitude near the $m = 1$ OLR is $\sim$2% at $0.1M_{\rm J}$ and increases by a factor ten to $\sim 20\%$ as the planet mass increase by a factor 10 to $1.0M_{\rm J}$, a perfect linear dependence. The direct proportionality continues even to the $2M_{\rm J}$ simulation with an amplitude 20 times that found at $0.1M_{\rm J}$. The maximum amplitude near corotation displays similar characteristics. For the $m = 2$ pattern, the maximum amplitudes near the ILR and CR increase in direct proportion to the planet mass, but the amplitude near the OLR saturates at $\sim 20 - 25\%$ for simulations with planets above $1M_{\rm J}$.

On the other hand, higher order patterns typified by $m = 10$ produce much different behavior. The amplitudes are not as large as for the $m = 1, 2$ patterns, and they no longer increase in linear fashion over the whole range. Instead, above $\sim 0.75M_{\rm J}$, the close correlation between the amplitudes for each of the three resonances is lost and the growth with planet mass appears to have saturated. Even below $0.75M_{\rm J}$ the increase is no longer directly proportional to planet mass. For example, a 2% perturbation increasing only a factor four with a factor 7.5 increase in planet mass. The mass at which saturation occurs is also similar to that for which the migration rate shown in figure 9 of Paper I undergoes its only real change in its behavior, from a slowly growing rate, to a completely flat function of planet mass. We conclude that the reason for this change is the saturation of the pattern amplitudes for the patterns most strongly affecting

the migration.

At the low end of the plot of mass vs. migration rate from Paper I (figure 9), an extrapolation of the migration rates to zero planet mass yields a non-zero rate. Such a phenomenon would appear to be either inconsistent with the view that the torques are dominated by Lindblad resonance interactions in the linear regime, or with the view that gravitational torques are responsible for the migration (since a zero mass planet would not generate such torques). Neither alternative can be fully supported. Instead, we favor the view that the simulations of the lowest mass planets (below $0.3 - 0.5 M_{\rm J}$) are in the linear regime, but that the true linear increase in the migration rate is not observed because of the positive torques due to low order m corotation resonances, and perhaps because of mixing between the torques from the CR and LRs of a given pattern (see discussion in section 3.4.2 below). More accurate quantification of the relative strength of the two sources of torques (from the CR and the LRs), must be done in order to determine the true migration rate of a planet.

3.3.3. The epicyclic frequency

In the theory of circumstellar disks, perhaps the two most critical parameters describing the problem are the natural resonance frequency of the system (the epicyclic frequency, $\kappa(r)$) and the driving frequency (the planet's orbit frequency, $\Omega_{\rm pl}$). The latter is very well determined since the planet is a single object. The former is more difficult due to the important effects of pressure and self gravity on the rotation profile. Nevertheless, a widely implemented approximation in theory is that the differences from true Keplerian orbits are small, so that the identity $\kappa(r) = \Omega(r)$ is approximately held. To what extent does the epicyclic frequency deviate from equality with the orbital frequency?

In figure 14, we show the ratio of the epicyclic frequency at each location in the disk to the orbital frequency Ω for the high resolution prototype simulations, with and without self gravity. The variation of κ is as large as 20% above and 10% below the orbital frequency at each radius in the disk for the self gravitating disk, but only ∼10% in the non-self gravitating disk. In the latter case, no gap is able to form due to the very rapid migration of the planet. In the former, the largest variation occurs about 2 Hill radii inward and outward from the planet, which corresponds to the positions of local minima in the surface density distribution in the nascent gap. Variation $> 5\%$ extends to a distance of 2 AU inwards and outwards of the planet and drops to a $\sim 2\%$ offset (due to the effects of pressure gradients and self gravity on the rotation curve) at locations further inward and outwards. Thus, although the equality between the two quantities is not exact, differences are larger than 20% nowhere in the disk and are 10% or less in most regions.

Differences of this magnitude remain important because as Ward (1997) and others have pointed out, the effect on the epicyclic frequency may be small but the effect on the gravitational torque suffered by the planet can be very large. Modifying the epicyclic frequency at each orbit radius will cause two separate modifications of the torque. First, the resonance positions will deviate from their Keplerian locations, and this change in position will affect the value of the gravitational potentials calculated at the resonance position. Second, the resonant denominator (for the LRs) and the Oort constant, B, (for the CR) may change their values from that predicted in an unperturbed disk. Are the differences in the epicyclic frequency from the orbital frequency large enough to affect strongly the values of these quantities?

3.3.4. The influence of the true rotation curve on the resonance positions

In figure 15, we show the resonance positions for all three resonances (ILR, CR and OLR) as a function of m, for the high resolution prototypes with and without self gravity. In only a few cases, do the true resonance positions correspond to the ideal Keplerian values. With self gravity, the CR positions are nearly coincident with the planet's orbit, while without it, they shift inward. At the same time, the LR positions are shifted due to the additional terms in the definition of the resonant denominator. Large m resonance positions follow closely the buffer region (of size $\sim 2H/3$) around the planet expected from the analysis of Artymowicz (1993a). Without self gravity the inner resonances shift inward by $\sim 1\%$, but the outer resonances remain largely unaffected because they are limited by the buffer region. For smaller m, the positions follow the ideal Keplerian positions more closely, but remain modified, especially for patterns $m \sim 10$. For these patterns, the resonance positions fall near the edges of the forming gap, which means that they will be disproportionately affected by large pressure gradients there.

If we follow instead the GT79 analysis and use the original definition of D of equation 5, small deviations from the Keplerian values are present both above and below the Keplerian values including self gravity, but in general the correspondence is quite close. Without self gravity, each of the resonances are systematically shifted inward by about 1% of the semi-major axis, which corresponds to about 20% of the Hill radius. The inner resonances are systematically shifted further away from the planet, while the outer resonances are shifted closer. Neither example displays the buffer zone expected from the use of equations 8 or 9.

3.3.5. The influence of the true rotation curve on $|rdD/dr|_L$.

The quantity, D, in equation 4, defines the strength and shape of the response of the disk to the perturbation from the planet. In combination with the torque cutoff function (equation 6), it determines the disk's response to the planet. In the interests of mathematical tractability, it is usually approximated by the first term in a Taylor series as $D \approx (rdD/dr)_{r_L} x$, where $x = (r - r_L)/r_L$, an approximation that in turn is often further approximated[4] as $rdD/dr|_{r_L} \approx -3(1 \mp m)\Omega^2_{r_L} \approx \pm 3m\Omega^2_{r_L}$, which is equivalent to the statement that the disk is Keplerian (i.e. $\kappa = \Omega$). To what extent are these approximations valid after the evolution begins?

The quality of the approximation may be measured by the ratio of the approximate value to the 'real' value obtained numerically from our simulations. A high value of the ratio means that more torques are produced for that pattern in the simulation compared to what would be predicted using the approximation. In figure 16, we show this ratio for both the inner and outer Lindblad resonances. For the self gravitating disk simulation, the approximation varies by up to a factor ~ 2.3 above and below the numerically obtained value for patterns with $m \lesssim 15$. Very sharp peaks exist in both the OLR and ILR ratios, coming at $m = 8$ and $m = 10$ for the OLRs and ILRs respectively. For the ILRs, the peak is broader and extends to $m = 15$. For lower m, the ratio drops below unity, indicating that the simulation produces less torque than expected. Above $m = 15$ and for both the ILR and OLR ratios, the approximation and the simulation produce very similar values, indicating that the approximation may be used without large errors in the torque.

In contrast, the non-self gravitating disk model shows differences only for the lowest m patterns. For $m > 10$ only relatively small deviations of order a few percent are present and no large peaks are present for

[4]We shall use the upper sign to refer to the ILR and the lower sign to refer to the OLR

any pattern although, as in the self gravitating version, the ratio increases to as high as 1.3 and as low as 0.8 for the lowest m patterns.

The patterns for which the approximation fails most severely (the ratio peaks) are those most sensitive to the structure of a gap. Their resonance positions tend to fall near the gap edges, both inside and outside the planet. Since the planet is nearer to the inner edge of the forming gap, more inner patterns, of higher order, are affected by its presence. For higher order patterns, where the resonance position falls well within the forming gap, the approximate form reproduces the simulation value to within a few percent. For the non-self gravitating simulation, the migration was so rapid that gap formation did not occur. The resonant denominator was therefore not strongly affected and the variations remained small.

3.3.6. The variation of Σ/B

The strength of the CRs is proportional to the gradient of Σ/B at the resonance, as indicated in equation 7. This quantity measures asymmetries in the circulation of matter as it travels on horseshoe orbits in the planet's vicinity (Ward 1991). For a Keplerian disk, the Oort constant reduces to $B = \Omega/4 \propto r^{-3/2}$. Since our assumed surface density is also a power law with the same proportionality, we expect that the value of Σ/B will be constant, and its gradient zero, making the CR torques insignificant. Clearly, torques from near the CR exist in our simulations. Is their origin due to the failure of this condition?

Figure 17 shows the ratio of Σ/B to its initial value as a function of radius in the region near the CR. The slope of this quantity presents a fair measure of the variation (i.e. the gradient) in Σ/B itself since the initial value is constant. In the self gravitating simulation, Σ/B decreases more than a factor two below its initial value within $\sim 2R_{\rm H}$ both interior to and exterior to the planet, while remaining nearly unchanged at the exact CR. The non self gravitating version displays variation of some 30% below its initial value and over a wider radial extent. The pattern is also offset relative to that seen with self gravity. While CR appears near a local maximum of Σ/B with self gravity, it appears near a local minimum without it. We speculate that this fact may simply be due to the very rapid migration in the latter case, so that the planet simply outruns the disk's ability to keep up.

While at the exact CR, the slope may indeed be relatively small, we recall the physical phenomenon of circulation on horseshoe orbits that gives rise to the CR torques in the first place. In that context, the conditions over the radial extent of the horseshoe orbit become important, and using the exponential term in equation 7 as our guide, we may associate the width of the resonance with the disk scale height. In both simulations, the Σ/B varies over a radial scale of 2–4 disk scale heights and over this range, the size of variation is as large as (or larger than) a factor of half its magnitude and takes both positive and negative sign. We conclude that evolution modifies the surface density and rotation profiles of the disk enough to lead to very large gradients in Σ/B, and will therefore also lead to significant CR torques.

3.4. The sensitivity of the torques to the various physical and numerical approximations

Figures 14–17 show that variations from the physical assumptions underlying the analytic derivations for the gravitational torques do occur. Each of the quantities probes a different aspect of the interaction, so that we can regard them as acting independently and test the sensitivity of the torque to each in turn. Which, if any, of the variations are important for correct evaluation of the torque? Similarly, which, if any,

of our numerical assumptions are important?

3.4.1. Torques at Lindblad resonances

Figures 18 and 19 show the torques as calculated under progressively less exact correspondence to equation 4, in which more precise quantities are cumulatively replaced with commonly used approximations. Significant differences in the one sided torque magnitudes occur when moving from nearly any panel to any other in either figure. The magnitude up or down of these variations is as much as a factor of several depending on the approximation. Since two one sided torques (each of opposite sign) must be added together, they produce a small net torque that can vary by a factor 3–10 and that can even change the sign of the torque for some patterns.

Even though the disk is highly stable against self gravitating instabilities (i.e. $Q > 5$ everywhere), the difference between the (a) and (b) panels of figure 18 shows that disk self gravity remains an important effect through the effective resonant denominator D_{sg}. A $\sim 20 - 30\%$ reduction in the calculated torques occurs when the self gravity term is suppressed (i.e. D_* is used instead). This difference occurs mainly because the positions of each resonance are shifted farther from the planet in the latter case. A second difference due to self gravity is that rotation curve itself shifts, so that the inner and outer resonances will be systematically shifted with respect to the planet (figure 15). The effect of this difference is clear when we examine the relative magnitudes of the torques from the (b) panels of figures 18 and 19. The outer (negative) torques on the planet are systematically larger in magnitude (more negative) without self gravity than with it.

The one sided torques for higher m patterns increase by 20% (or more for the highest m's) in panel (c), relative to (b), where we substitute the torque cutoff function and D for the generalized Laplace coefficients and D_*. The physical interpretation of this replacement lies in how the three dimensional disk potential (implied in the generalized Laplace coefficients) and non-WKB terms are accounted for in the derivation. The change in one sided torques leads to a factor ~ 3 increase in the calculated net torque on the planet, which is quite consistent with the analytic discussion of the effect predicted for this replacement discussed by **?**)][see esp. his figure 1]art93b. Together, the generalized Laplace coefficients and the resonance buffer region act very effectively to suppress the torques for high m patterns.

For the non self gravitating version, another change is much more dramatic. The outer torques (especially for higher m) increase in magnitude by as much as a factor 10, while the inner torques remain essentially unchanged. The primary culprit in this case is the resonance position shifts, due to the replacement of D_* with D as resonant denominator. When the buffer region produced using D_* is suppressed, both the inner and outer resonances are shifted inward relative to those in the self gravitating disk, with the outer resonances being closer to the planet (producing a larger torque). The inner resonances are shifted inward relative to the Keplerian positions, but end up being shifted nearly to what were their buffered positions, and are therefore not greatly affected.

If we account exactly or approximately for local variation in the rotation profile (i.e. variation in $|rdD/dr|_{r_L}$ from figure 16), we find large changes in the one sided torques for patterns with $m \approx 7 - 12$, due to the small scale rotation curve variation near the forming gap edges. When we replace the true (first order approximation of the) resonant denominator with its approximate form, $-3(1 \mp m)\Omega^2_{r_L}$, in panel (d), the peaks become much less significant. The torques in figure 19(d) show no features comparable to those in figure 18(d), because gap formation is much less advanced and little variation in the resonant denominator exists. Therefore we conclude that self gravity plays only an indirect role in the variation of the resonant

denominator, through the effect the migration rate has on the disk profile.

Even though m to m variations are present in the torques from the simulations, no variations of similar magnitude to those from the analytic calculations shown in figure 18(a)–(c) are present. The answer to this apparent paradox becomes clearer upon examination of figure 12. The response of the disk (i.e. the torques) occurs over about 1/2 cycle of the wave rather than at a single radius, and the shape of the response varies with each pattern. We conclude that in order to account for this spatial variation, either an average which adequately accounts for the variation or terms of higher order than the first order approximation currently implemented must be used. Perhaps surprisingly, the approximation $|rdD/dr|_{r_L} = -3(1 \mp m)\Omega^2_{r_L}$ appears to be such an average, at least for the patterns affected most by gap formation ($m \approx 10$). The same conclusions may remain somewhat useful for use in conjunction with the modified resonant denominators, D_{sg} or D_* as well, in spite of the fact that use of this approximation is only justified in combination with the torque cutoff function, because the differences are small when m itself is not too large (specifically for the patterns affected most by the gap edge pressure gradient effects). Due to space limitations, we have not discussed another common approximation of the resonant denominator, as $rdD/dr|_{r_L} = \mp 3m\Omega^2_L$. However, we note that this approximation also leads to net torque changes of a similar magnitude to the others in panels (d)-(f).

Accurate or approximate determination of the resonance positions provides an additional significant source of variation in the calculated torques. Figures 18(e) and (f) shows two approximations of the resonance positions. Panels (e) show the effect of replacing the position determined by the 'zero' of the resonant denominator with exact $(m \pm 1)/m$ ratios to the orbit frequency. Changes of almost a factor two occur in the self gravitating disk net torques. In the non self gravitating disk only small differences occur, presumably due to the already very large shifts from other sources. This replacement is equivalent to saying that $\kappa = \Omega$ everywhere, which we have shown in section 3.3.3 to be accurate to 20%. In the (f) panels, we show effect of another approximation of the resonance positions, namely that the argument of the Bessel functions (see equation 10), $m(1 - r_L/a)$, is exactly 2/3. While the torques are affected only at the $< 5\%$ level by the Bessel function approximation itself, a change of order unity is seen in the resulting torques on the planet when its argument is approximated.

Based on the changes we observe when we implement various approximations, we can make several important conclusions. First, and most importantly, the torque calculations are exquisitely sensitive to nearly all of the common approximations used to calculate them. Qualitatively and quantitatively incorrect results will be obtained unless rigid adherence to the mathematically derived formulation is strictly observed, and a physically inclusive model is developed. Second, a theoretical model specifically including disk self gravity is important for correct evaluation of the torque, even in disks where self gravitating spiral density waves are largely suppressed (i.e. $Q >> 1$ everywhere) because it acts to shift the resonance positions. Third, use of the torque cutoff function may be completely avoided when both the resonant denominator is modified according to equation 9 and the Laplace coefficients are modified according to equation 11. We would caution that such a replacement may be of limited value however, since the true vertical structure of the disk (modeled with the generalized Laplace coefficients) remains an approximation.

3.4.2. The LR torque magnitude differences, and an attempt to obtain correspondence

Even when each of the approximations in section 3.4.1 are accounted for, the predicted torques do not reproduce those obtained from the simulations, which we saw were a factor 3–6 smaller than predicted. In very recent work, D'Angelo, Henning & Kley (2002) have also reported a similar discrepancy between

analytic predictions and simulations, including for planet masses far below those in our own study, for which perturbations are very small and simulations are very far from any possible non-linear effects. They implement a nested grid method to obtain extremely high resolution of the mass in two dimensions around the planet, and consider a gravitational softening smaller than ours. What is the origin for this large difference, occurring in both results?

It is possible to eliminate the effects of both finite grid resolution and gravitational softening as a cause for the differences. D'Angelo, Henning & Kley (2002) provide extremely high grid resolution near the planet and experience the same phenomenon, while gravitational softening is accounted for theoretically through our implementation of the generalized Laplace coefficients from equation 11. Instead, we suggest that the origin of the differences may be another consequence of the finite width of the resonances (recall also the discussion of the resonant denominator, in section 3.4.1, above).

In a derivation resulting in the same torque formulae for LRs originally developed by GT79, **?**)][hereafter MVS]MVS87 define expressions for the resonance width in a disk with pressure, self gravity or viscous forces (or any combination) acting on the fluid. As a condition of validity, they point out that the resonance must be narrow compared to the distance between the resonance and the planet (in non-dimensional form $w << 1/m$, with $wa_{\rm pl}$ the true width) so that the orbits of the planet and resonating material do not cross. This condition is equivalent to the tight winding approximation used in the torque derivation. They suggest that failure of this criterion will lead to mixing of the torques from inner and outer resonances and a decrease in the torque exerted.

MVS derive a width for a Lindblad resonance of

$$|w|^3 = \frac{c^2/\Omega_{r_L}}{3mr_L^2\Omega_{\rm pl}} \tag{17}$$

assuming that pressure dominates over self gravity and viscosity. Substituting values for the variables appropriate for our simulations, we find that $w \approx 0.1m^{-1/3}$. For $m = 10$ and $m = 20$, we thus obtain $w \approx 0.045$ and $w \approx 0.037$ respectively, which is comparable to the distance between the planet and the resonance and suggests that some overlap and mixing may occur for these patterns. Further, if mixing between the LRs and CR can occur (as we discuss in the following section), then the amount of overlap will be larger since the distances are smaller.

There are several important caveats to consider before this conclusion can be substantiated however. First is the fact that the pressure wave propagates *away* from CR, and so has very low amplitude close to the planet available for mixing. The self gravity term will be responsible for a second wave in the disk which propagates towards the CR. Its width (from the MVS formulation) is $w \sim 7 \times 10^{-2}m^{-1/2}$ in our simulations, nearly as large as the pressure term. It is interesting to speculate that this term could also be active, though there is no direct evidence for it.

Secondly, as discussed in section 3.3.4, the LRs will shift due the addition of non-WKB terms, neglected in the MVS analysis. Indeed, the entire derivation of MVS is superseded by the later Artymowicz (1993a) analysis, in which the issue of the resonance widths was not specifically addressed. Close examination of figure 15 shows that the buffer zone does not begin to modify the resonance positions until $m \approx 20$, so if we naively use the resonance widths from the WKB theory with the resonance positions from the non-WKB theory, we still may find significant overlap, though less than might originally be expected from the MVS analysis.

It is beyond the scope of this work to investigate further the possibility that the differences between

theory and simulation are due to resonance overlap or to some other effect. However, it may still be useful to obtain information about the character of the differences for future investigations. We saw in Paper I that the simulations were in fact very sensitive to the softening implemented in the simulation. Here we ask a similar question about the torques from the analytic derivations. We attempt to obtain the best correspondence possible between the simulation and theoretical torques, by adjusting the available parameters in the analytic theory.

Figure 20 shows the analytic predictions torques for the self gravitating simulation, assuming a gravitational softening factor 2.5 larger than was actually present in the simulation itself. We also use the approximated resonant denominator, $-3(1 \mp m)\Omega_L^2$ for patterns with $m \leq 15$, but retain its numerically derived value for higher m patterns. In both the self gravitating and non self gravitating versions, the inner (positive) torques are reproduced much more faithfully than the outer (negative) torques especially without disk self gravity. Overall, except for very high m patterns, where the analytic torques underestimate those from the simulations due to the increased softening, the agreement is within $\sim 20\%$ for any given pattern in the self gravitating simulation.

It is an encouraging sign for the theory that we are able to reproduce the behavior of the $m \leq 15$ patterns, since those are the ones for which the resonant denominator is most strongly affected by the forming gap and for which the variation in softening will have the least effect. However, the non self gravitating version fares much worse, with large differences for nearly all patterns. Thus these after the fact parameter adjustments should carry little weight.

3.4.3. Torques at Corotation

As we noted above, the torques due to interactions at the CR are characterized at least as well by their differences from simulation to simulation than by their similarities. Except to say that they are significantly nonzero, we were unable to determine accurately their magnitude due to our limited spatial resolution. What conclusions can be made about the importance of the interactions at corotation based on the causes of these variations in our simulations?

Both with and without disk self gravity, the CR position is very close to the planet, making quite large torques possible. In fact, the position in the self gravitating disk version is very nearly coincident with the planet's orbit radius. With self gravity suppressed it lies further inward. In spite of its greater distance, the CR torques are larger in the non self gravitating versions, so the separation between the CR and the planet is not by itself the determining factor in the torque magnitude.

The torque produced at corotation is exerted within a distance of a few scale disk heights of the resonance (see the exponential term in equation 7), but its theoretical magnitude is determined only at one point in that range–the exact resonance position. Therefore, while the analytic derivations account for the width of the resonance they do not account for large variations in the disk quantities over the spatial scale where the torques are active. Variations in these quantities (e.g. Σ/B) of order unity are present over these same few disk scale heights. Further, as Korycansky & Pollack (1993) also point out in a much different analysis, the planet's gravitational potential may also vary significantly over the same spatial scale. Both issues will render attempts to compare to theory of limited use, and we conclude that the approximation that the conditions only at the exact resonance define the torque cannot be supported for corotation resonances. Figures 7 and 8 showed that both sign changes and large magnitude changes in the torque do occur over this same range, strengthening this conclusion.

In some sense, the quantity Σ/B is a measure of the flow pattern of mass around the planet. Lubow, Siebert & Artymowicz (1999) studied the mass flow around the planet during the Type II migration period at a factor ∼20 higher resolution than our simulations and showed that mass transfer through the gap can occur efficiently. They also find that a circumplanetary disk develops and a large amplitude, double armed spiral pattern forms within it. The mass transfer they see will inevitably lead to a net torque on the planet, and as they discuss, the net torque from the small radial region around the planet is as large as that from the rest of the disk. Presumably, the contribution during Type I migration will only be larger, making CR torques even more important for the migration than they indicate. However, the conditions in their work are dissimilar from our own in a very significant way–we showed in section 2.2 that a circumplanetary disk was very unlikely during Type I migration. How much will the flow pattern and torques during the Type I period change due to the existence of a (properly resolved) rotating envelope structure rather than a disk?

Although we quite naturally expect CR torque to be sensitive to the r coordinate, sensitivity in the angular coordinate is missing in equation 7. In separate analyses (Ward 1991; Masset 2001; Balmforth & Korycansky 2001), the sensitivity of the CR torque to the angular coordinate is recovered in the context of angular momentum exchange between the planet and disk material in the horseshoe region of the disk. However, these authors also conclude that the CR torques will not in the end be very important because the circulation around the horseshoe orbits will reach a steady state in a relatively short time and so the torques will decrease to zero. Is the fact that we start without a saturated circulation region the reason that the CR torques are large in our models?

A possible 'escape route' for the saturation argument has been that if the planet migrates, then the region affected by the CR torques will continually change and the saturation will never occur. While this may still be true, we believe there is an equally plausible alternative mechanism–namely the changes in the disk's radial profile caused by the actions of the Lindblad resonances. The question is relevant because as we concluded above, the CRs act over a finite region (of a few disk scale heights) that overlaps with the higher order m LR locations. If the LRs can produce changes in the disk profile on a similar or shorter time scale to the one at which CR interactions smooth them out, then saturation will never occur. **?**)][see esp. their figure 8]BK01 showed that the time scale for saturation is

$$\tau_{\rm CR} \approx \frac{5P}{2\pi}\sqrt{\frac{M_\odot}{M_{\rm pl}}}, \tag{18}$$

where P is the planet's orbit period. A relevant quantity for the LRs is the gap formation time scale (Bryden *et al.* 1999)

$$\tau_{gap} = P\left(\frac{M_\odot}{M_{\rm pl}}\right)^2\left(\frac{\Delta}{a_{\rm pl}}\right)^5 = 3^{-5/3}P\left(\frac{M_\odot}{M_{\rm pl}}\right)^{1/3} \tag{19}$$

where the right hand equality is obtained from setting the gap width, Δ, equal to the Hill radius, where most of the LR positions are found. Relating these two quantities to each other yields

$$\tau_{\rm CR} = 3^{5/3}\frac{5}{2\pi}\left(\frac{M_\odot}{M_{\rm pl}}\right)^{1/6}\tau_{gap}. \tag{20}$$

The saturation time scale for the CRs is thus comparable to or larger than the gap opening time scale for Jovian and sub-Jovian mass planets and the CRs will always be active.

4. Discussion and Comparisons to Other Work

In this section we attempt to compare our results with some of what has gone before, to place them in context. Many previous numerical studies of disks with embedded planets have also included mass accretion onto the forming planet. Some have begun, as we do, with an unperturbed disk (Bryden *et al.* 1999; R. P. Nelson *et al.* 2000), while others begin with an already formed gap (Lubow, Siebert & Artymowicz 1999; Kley 1999; Kley, D'Angelo & Henning 2001). One study concentrates on very high resolution local simulations of a small region of the disk containing the planet (Miyoshi *et al.* 1999). In many instances these studies have also suppressed migration in order to explore the gap formation and accretion processes in isolation.

Similar to Bryden *et al.* (1999) and Lubow, Siebert & Artymowicz (1999), we find that matter accretes primarily from inside and outside the planet's orbit, rather than from the region radially closest to the planet. The planet masses reached at the end of our accretion simulations are similar to those of found by others, but the accretion rates in our simulations are much larger than those of the previous work. The differences in the time scales are dominated by the differences in assumptions about the initial conditions–they start with a nearly empty gap region, while we do not. Secondarily, their simulations assume that accreted mass does not accumulate on the planet–its mass remains constant–since they were primarily interested in studying the properties of the flow through the gap. Common to both our models and theirs is that the planet accretion is self limiting. Planet apparently cannot accrete more than $\sim 5 - 10 M_{\rm J}$ of mass from the disk starting either from the initial condition of an unperturbed disk or from one with an already formed gap, because additional mass is driven away by dynamical torques.

This conclusion is interesting on both theoretical and observational grounds. Specifically, Jovian planet growth was long thought to be a self limiting process due to gap formation (Lin & Papaloizou 1993), but recently had been challenged by the possibility of mass accretion through the gap (Bryden *et al.* 1999; Kley 1999; Lubow, Siebert & Artymowicz 1999). Our combined results show that while growth and accretion continues with or without a gap, there is a clear limit to this process, no matter what initial conditions (gap/no gap) are used. On the observational side, the masses reached by our simulations and Kley's are interesting because they are comparable to the largest 'minimum masses' (i.e. $M \sin i$) observed for low mass companions in short period orbits around other stars.

Our results for the sign of the accretion torque are opposite those of R. P. Nelson *et al.* (2000), who show that accreted matter brings with it net positive angular momentum. Our work shows net negative angular momentum accretion. While our conclusion and theirs are the same–that the influence of accretion torques on the migration are small–the difference in sign of the torque is troubling. There are a number of differences in the disk morphologies, which could affect the result. In particular, the surface density distribution we use is steeper than theirs, going as $r^{-3/2}$ rather than the flat, r^0 profile they use. It seems quite plausible that with such distribution the amount of matter accreted from outside the planet's orbit (i.e. with greater angular momentum) will be higher than with a steeply decreasing profile, causing the sign of the net accreted torque to be positive.

Our *acc0* and *acc1* simulations (with accretion factor, $f = 1.0$ and 0.1, respectively) have very similar initial conditions and physical assumptions to those discussed in Armitage & Hansen (1999), except that their disks were about twice as massive as ours, and their interest was on triggering further planet formation rather than migration. Nevertheless, the outcomes are fundamentally quite different. They find that rapid growth of the planet (from $1 M_{\rm J}$ to 4-5$M_{\rm J}$ in less than 30 yr) ends in fragmentation of the growing spiral structure into additional planetary mass companions in fewer than 3 orbits of the original planet. While

we also find rapid spiral structure growth as the planet gains mass and perturbs the disk, we do not find any signs of the fragmentation they observe. In work in preparation (Nelson 2003), we show that their fragmentation is instead numerically induced by a violation of a two dimensional version of the Truelove *et al.* (1997) criterion applicable in disks. This condition is satisfied in our simulations, which do not fragment.

In general, each of the numerical works above focus their attention on the phenomenological aspects of the evolution (gap formation, accretion processes) and spend much less effort in direct comparisons with theory. In our work, we have made a detailed comparison of the results of our simulations and the theoretical predictions for both Lindblad and corotation interactions. We have attempted to examine the assumptions underlying the development of the analytic torque formulae, that are made in order to make the problem tractable enough to solve mathematically. The theoretical work to which we compare is based on the seminal studies of GT79, GT80 and Lin & Papaloizou (1979) and have in general focused either on effects that determine the Lindblad torques (Lin & Papaloizou 1986; Meyer-Vernet & Sicardy 1987; Ward 1986; Artymowicz 1993a) and the formation of the gap (Takeuchi *et al.* 1996; Ward 1997), or on the character of the corotation torques Ward (1988, 1991); Masset (2001); Balmforth & Korycansky (2001).

Many of the qualitative predictions of the theories are reproduced in our simulations. We find that dynamical torques develop exhibit wavelike radial structure that decays with distance from the planet in the regions dominated by Lindblad interactions, and non-wavelike structure close to the planet where corotation resonances are strong. Since the Lindblad interactions are sums of two terms from the inner and outer resonances (except $m = 1$) with opposite sign, the net contribution from any given spiral wave pattern, m, is much smaller than from any single resonance considered in isolation.

When we look in more detail however, correspondence is weaker. The expected linear dependence of the migration rate on planet mass is not reproduced (see Paper I) and the torque magnitudes from Lindblad resonances obtained from the simulations are a factor 3-6 smaller than those predicted from theory. Secondly, specific features of the torques as a function of pattern number m do not correspond well in most approximations, especially for patterns whose resonances fall near the edges of the forming gap.

Two of the most critical assumptions made by GT79 are that the interactions produce perturbations in the disk that are small so that linear theory may be applied, and that all interactions between the disk and planet occur exactly at either a Lindblad or corotation resonance. We have checked both of these assumptions in our simulations and have found that they can be supported, at least in part, for planets with mass $M_{\rm pl} \lesssim 0.5 M_{\rm J}$. For these models, the perturbation amplitudes at each resonance are proportional to the planet mass, which agrees with the assumption that the perturbations in the disk should be linearly proportional to the size of the perturber. For higher mass planets, the pattern amplitudes of the most important patterns ($m \sim 10 - 20$) become saturated and no longer vary as a function of planet mass. Computations that depend on the validity of the torque formulae for these masses may suffer from inaccuracy.

While it is true that some torque is exerted far from the resonances in our simulations (and indeed, is expected–see e.g. Ward (1986)), we do find that by far the largest fraction of the torque from any given pattern is exerted over the first cycle of the wave at a Lindblad resonance. This validates in part the analytic derivation of the angular momentum flux discussed in GT79, which depended on the planet's potential varying little near the resonance and the tight winding assumption. A closer examination however, shows that we cannot completely validate the mathematical derivation in our simulations because the width of the resonance is not negligible, and the shape of torque response within that resonant width varies from one pattern to the next, making a determination of the true effective resonance position difficult.

This variation is especially important in the context of approximations of those positions made to ease

calculation of the torques. We have shown that small shifts in the resonance positions can have a very large effect on the calculation of the torque on the planet. The fact that shifts due to pressure gradients could produce large changes in the torque is well known (Artymowicz 1993a; Ward 1997), but we are not aware of any work (analytic or numerical) that considers the shifts due to disk self gravity. Our results indicate that the shifts due to self gravity are approximately the same magnitude as those caused by pressure gradients, but opposite in direction. Migration rates are much slower including disk self gravity than without it.

Of particular interest in our torque comparison is the fact that torques from the simulations are a factor of 3–6 smaller in magnitude than those from analytic models that include the effects of vertical structure and the buffer region around the planet, as outlined by Korycansky & Pollack (1993); Artymowicz (1993a,b); Miyoshi *et al.* (1999). Indeed, the difference is compounded on top of another factor ~ 3 decrease from models that use the original torque cutoff function without the buffer region.

Recent work by D'Angelo, Henning & Kley (2002) has also studied the migration rates for a range of planets from a few earth masses up to Jovian mass objects. They also find that the migration rates from their simulations fall a factor of several smaller in magnitude than the predictions of theory. Given that the magnitude discrepancy has been found by separate workers, using completely independent numerical codes, we would speculate that it is a real effect. Regardless of the origin, the conclusions reached in Paper I only become stronger if the torques are instead much larger than in our simulations.

D'Angelo, Henning & Kley (2002) briefly speculate that the reason for the discrepancy is the existence of positive corotation torques on the planet, which act to reduce the net migration rate. The results of our work would seem to refute this supposition because we have separated out the contributions due both to LR and CR torques and found that the torque magnitude discrepancy exists in the LR torques independent of the CR torques. The comparison between our work and theirs is particularly interesting because the magnitude discrepancy extends to very small planet masses, for which the system is certainly in the linear regime. A linearized, numerical study using an iterative techniques (Korycansky & Pollack 1993) has studied the effects of both LR and CR torques, while avoiding some of the approximations made in the purely analytic work. In contrast to our results and D'Angelo, Henning & Kley (2002), they report good agreement between analytic theory and their numerical model for LR torques, especially for patterns for which the torque cutoff function does not play a role. Their net LR torques were accurate to $\lesssim 50\%$, as opposed to the factor 3–6 discrepancy that we find.

Comparison of the three results is somewhat puzzling because all three (Korycansky & Pollack (1993), D'Angelo, Henning & Kley (2002) and our study) consider two dimensional systems and include gravitational softening (though with varying amounts) and would therefore seem to solve the same physical problem and be expected to yield the same results. It is interesting to speculate that the differences between theory and simulation found by us and D'Angelo, Henning & Kley (2002) are due to the finite width of the resonances and/or to resonance mixing, which causes one resonance and another to partially cancel each other's torques, as discussed in MVS. Such resonance mixing would be still more efficient if the corotation resonances (not considered in the MVS analysis) participated in the effect, since the inter-resonance distance is smaller and the overlap is greater. No proof of this supposition can be found in our simulations however.

It is also interesting to speculate that any resonance mixing phenomena that are present may be due to a breakdown of some of the most basic assumptions of resonances themselves. In simplest picture of a resonant interaction of any kind, a particle is bound and oscillates in a parabolic potential, driven by a small external force. Applied to a star/planet/disk system, the (now approximately) parabolic potential is a sum of several terms, including a stellar potential and an centrifugal 'effective potential' term that accounts for

the conservation of angular momentum. In cases with $M_{\rm pl}$=$0.1-1M_{\rm J}$ as in our study and many others, the driving term (interaction with the planet) will no longer be small, especially in the case where the planet and disk matter are within a few Hill radii of each other. Indeed, the original potential may be perturbed so strongly that it may no longer be parabolic at all. Such a condition is certainly true any time the resonance position falls closer than one Hill radius from the planet, where disk matter may no longer even remain bound in the unperturbed potential, and may be true in more limited circumstances at much larger distances.

In addition to the LR torques, we also find significant torque contributions due to corotation resonances. A partial sum of the torques from these patterns ($m \leq 15$), is smaller in magnitude than the net LR torque but is opposite in sign (positive) and large enough to decrease the total net torque on the planet by 20-30%, below that due to the LRs alone. Our results are in qualitative agreement with Korycansky & Pollack (1993), who found CR torques that were opposite in sign from the LR torques for small m. Their results produced LR and CR torques with comparable magnitude for a uniform surface density disk, but in a disk where the gradient of Σ/B was zero, produced no CR torques, as expected. While our models begin with the same initial condition, they quickly evolve away from it and large gradients develop, allowing torques to develop.

If, as we have concluded, a large fraction of the gravitational torque on the planet is exerted within one or a few Hill radii of the planet, then it will be critical to resolve the three dimensional mass distribution there in order to understand the global problem of the planet's migration through the disk. Two distinct problems are associated with this region. First, with the possible exception of the recent D'Angelo, Henning & Kley (2002) work in 2d, no present models have resolved the region within a few Hill radii of the planet well enough to determine the gravitational torques with sufficient precision to make an accurate determination of the migration rate. The full, three dimensional mass distribution must be specified in order for such a determination to be made. This description will require not only high spatial resolution, but also a better thermodynamic model, since energy release during the mass accretion will affect the thermodynamic structure near the planet, changing the mass distribution.

Second, no current models have made an accurate determination of the mass accretion rate onto the planet during the Type I migration era. This is important for the migration because it determines how rapidly the planet can grow large enough to open a gap via dynamical processes. The mass accretion rate will be better known when models that resolve the flow pattern and the thermodynamic state of the region within a few Hill radii of the planet are developed. Improving the description of the flow pattern will help to determine the angular momentum input into the envelope and the likelihood of rotational instabilities as it grows. Improving the thermodynamic description of the gas will help to determine the mass accretion rate into the envelope itself, and the frequency of those instabilities if indeed they can grow. Work is now underway that will begin to address both of these questions.

We would like to thank Willy Kley and Pawel Ciecielag for many productive conversations during the evolution of this work. Bill Ward, Pawel Artymowicz and Doug Lin each provided very helpful discussions about the details of the torque calculations and Adri Olde Dalhuis pointed out the work of Olvers (1967), which improved the accuracy of our calculation of the Laplace coefficients. AFN thanks the UK Astrophysical Fluids Facility (UKAFF) for support during the last months during which this manuscript was prepared. Some of the computations reported here were performed using the UK Astrophysical Fluids Facility (UKAFF).

REFERENCES

Armitage, P. J., Hansen, B. M. S., 1999, Nature, 402, 633

Artymowicz, P., Lubow, S. H., 1993, ApJ, 419, 155

Artymowicz, P., 1993, ApJ, 419, 166

Balmforth, N. J., Korycansky, D. G., 2001, MNRAS, 326, 833

Bodenheimer, P., Pollack, J. B., 1986, Icarus, 67, 391

Bryden, G., Chen, X., Lin, D. N. C., Nelson, R. P., Papaloizou, J. C. B., 1999, ApJ, 514, 344

Bryden, G., Lin, D. N. C., Ida, S. 2000, ApJ, 544, 481

D'Angelo, G., Henning, T., Kley, W., 2002, A&A, 385, 647

Frank, J., King, A., Raine, D., 1992, Accretion Power in Astrophysics, ch. 5.6, Second Edition, Cambridge University Press: Cambridge

Goldreich, P., Tremaine, S., 1979, ApJ, 233, 857 (GT79)

Goldreich, P., Tremaine, S., 1980, ApJ, 241, 425 (GT80)

Kley, W., 1999, MNRAS, 303, 696

Kley, W., D'Angelo, Gennaro, Henning, Thomas, 2001, ApJ, 547, 457

Korycansky, D. G., Bodenheimer, P., Pollack, J. B., 1991 Icarus, 92, 234

Korycansky, D. G., Pollack, J. B., 1993, Icarus, 102, 150

Masset, F. S., 2001, ApJ, 558, 453

Lin, D. N. C., Papaloizou, J. C. B., 1993, In Protostars and Planets 3, ed. Lunine, J., and Levy, E., University of Arizona Press: Tucson

Lin, D. N. C., Papaloizou, J. C. B., 1979, MNRAS, 186, 799

Lin, D. N. C., Papaloizou, J. C. B., 1986, ApJ, 309, 846

Lubow, S. H., Siebert, M., Artymowicz, P. 1999, ApJ, 526, 1001

Meyer-Vernet, N., Sicardy, B., 1987, Icarus, 69, 157 (MVS)

Miyoshi, K., Takeuchi, T., Tanaka, H., Ida, S., 1999, ApJ, 516, 451

Nelson, A. F., Benz, W., 2002, ApJ, submitted (Paper I)

Nelson, R. P., Papaloizou, J. C. B., Masset, F., Kley, W., 2000, MNRAS, 318, 18

Olvers, F. W. J., 1967, Journal of Research of the National Bureau of Standards, 71B, 111

Pickett, B. K., Durisen, R. H., Davis, G. A., 1996, ApJ, 458, 714

Pollack, J. B., Hollenbach, D., Beckwith, S., Simonelli, D. P., Roush, T. & Fong, W., 1994, ApJ, 421, 615

Shu, F. H., 1992, The Physics of Astrophysics, Volume II: Gas Dynamics, University Science Books: Mill Valley

Takeuchi, T., Miyama, S. M., Lin, D. N. C., 1996, ApJ, 460, 832

Toman, J., Imamura, J. N., Pickett, B. K., Durisen, R. H., 1998, ApJ, 497, 370

Truelove, J. K., Klein, R. I., McKee, C. F., Holliman, J. H. Howell, L. H., Greenough, J. A., 1997, ApJ, 179

Ward, W. R. 1986, Icarus, 67, 164

Ward, W. R. 1988, Icarus, 73, 330

Ward, W. R. 1991, Lunar and Planetary Science Conference, 22, 1463

Ward, W. R. 1997, Icarus, 126, 261

Wuchterl, G., 1991, Icarus, 91, 31

AAS LaTeX macros v5.0.

Table 1. Initial Parameters For Simulations

Name	Resolution $(r \times \theta)$	Disk Mass $M_\odot$	Planet Mass M_J	Softening ϵ	Accretion Factor, f	Duration (yr)
acc0	128×224	0.05	0.30	1.0	1×10^{0}	1800
acc1	128×224	0.05	0.30	1.0	1×10^{-1}	1800
acc2	128×224	0.05	0.30	1.0	1×10^{-2}	1800
acc3	128×224	0.05	0.30	1.0	1×10^{-3}	1800
acc4	128×224	0.05	0.30	1.0	1×10^{-4}	1800
gap0[1]	128×224	0.05	0.30	1.0	1×10^{0}	1800
gap1[1]	128×224	0.05	0.30	1.0	1×10^{-1}	1800
gap2[1]	128×224	0.05	0.30	1.0	1×10^{-2}	1800
gap3[1]	128×224	0.05	0.30	1.0	1×10^{-3}	1800
gap4[1]	128×224	0.05	0.30	1.0	1×10^{-4}	1800
mas3	128×224	0.05	0.30	1.0	0.0	3000
Sof7	256×448	0.05	0.30	2.0	0.0	2400
nosg[2]	128×224	0.05	0.30	1.0	0.0	1200
Nosg[2]	256×448	0.05	0.30	2.0	0.0	500

[1]The simulations *gap0–gap4* are identical to *acc0–acc4* except that they begin with a gap formed by evolving the system for 3000 yr with the planet's migration and accretion suppressed.

[2]The simulations *nosg* and *Nosg* do not include self gravity in the disk, but are otherwise identical to simulations *mas3* and *Sof7*, respectively.

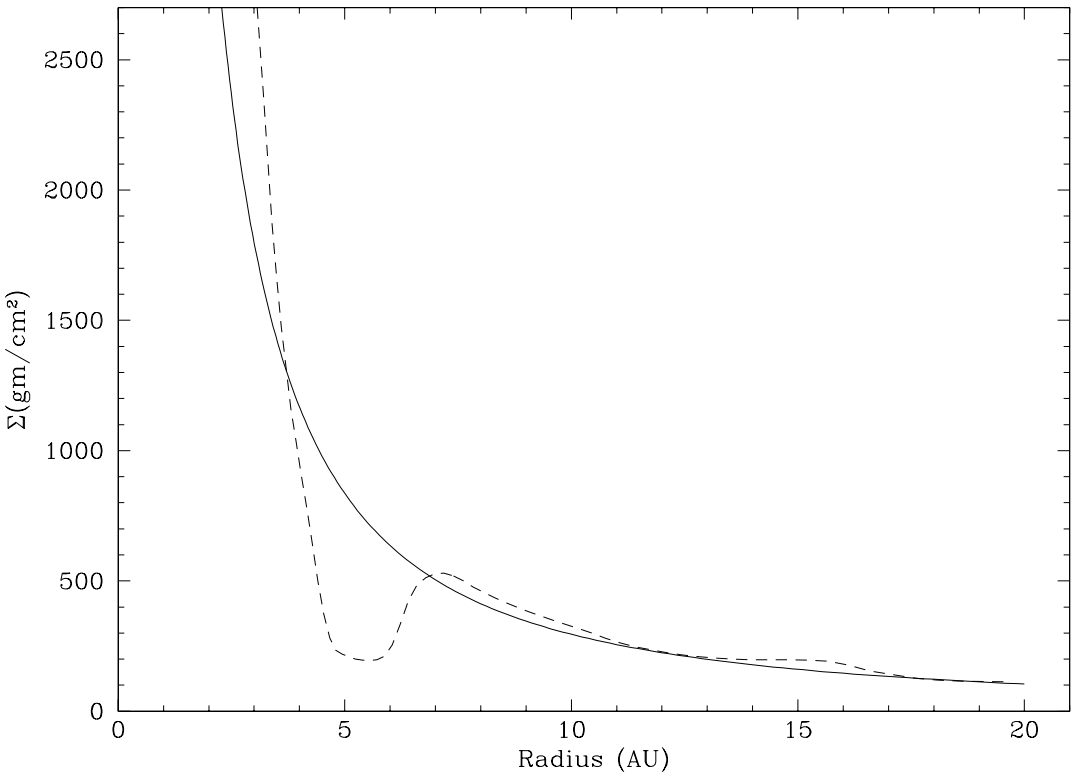

Fig. 1.— Initial conditions for surface density of the disk. The dotted vertical lines denote the inner and outer grid boundaries. The dashed line defines the azimuth averaged density distribution of the initial conditions for the *gap* series of simulations, defined in the text.

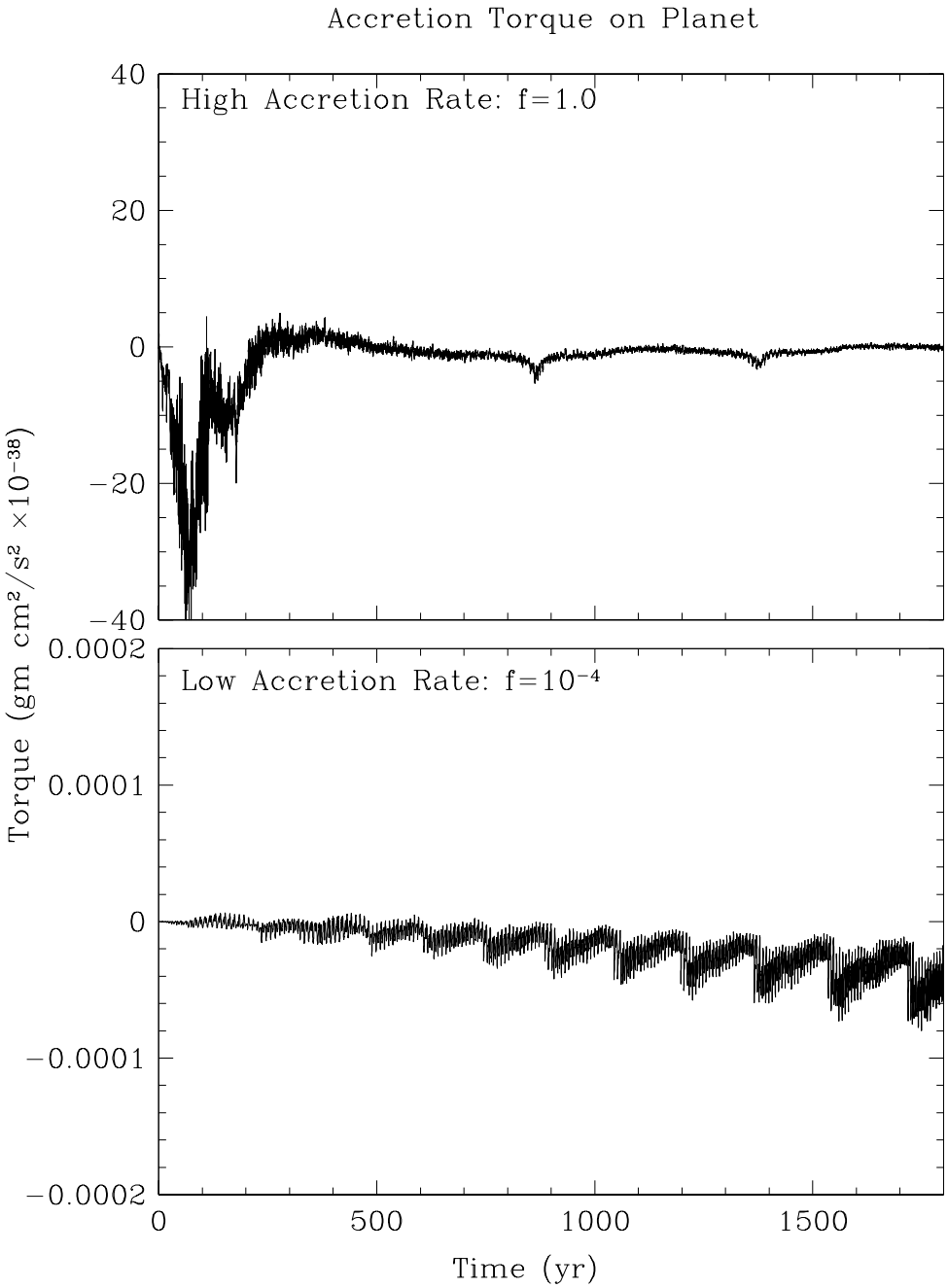

Fig. 2.— Contribution to the dynamical torque due to the accretion of matter onto the planet. Top: the torque for the no initial gap model, *acc0*, with $f = 1.0$. Bottom: the torque for the $f = 0.0001$ model, *acc4*. In each case, although the magnitudes of the torques due to mass accretion are different, their signs are the same. Mass accretion provides a net, negative torque on the orbital angular momentum of the planet. In each case, the torque is smoothed using the average torque in a moving 0.1 yr window, in order to average out the short term effects of our finite grid resolution. The periodicity in the *acc4* model is due to the passage of the planet through successive rings of grid zones as it migrates inward towards the star. Its long term negative slope is due to the increase in mass of the planet (see equation 3).

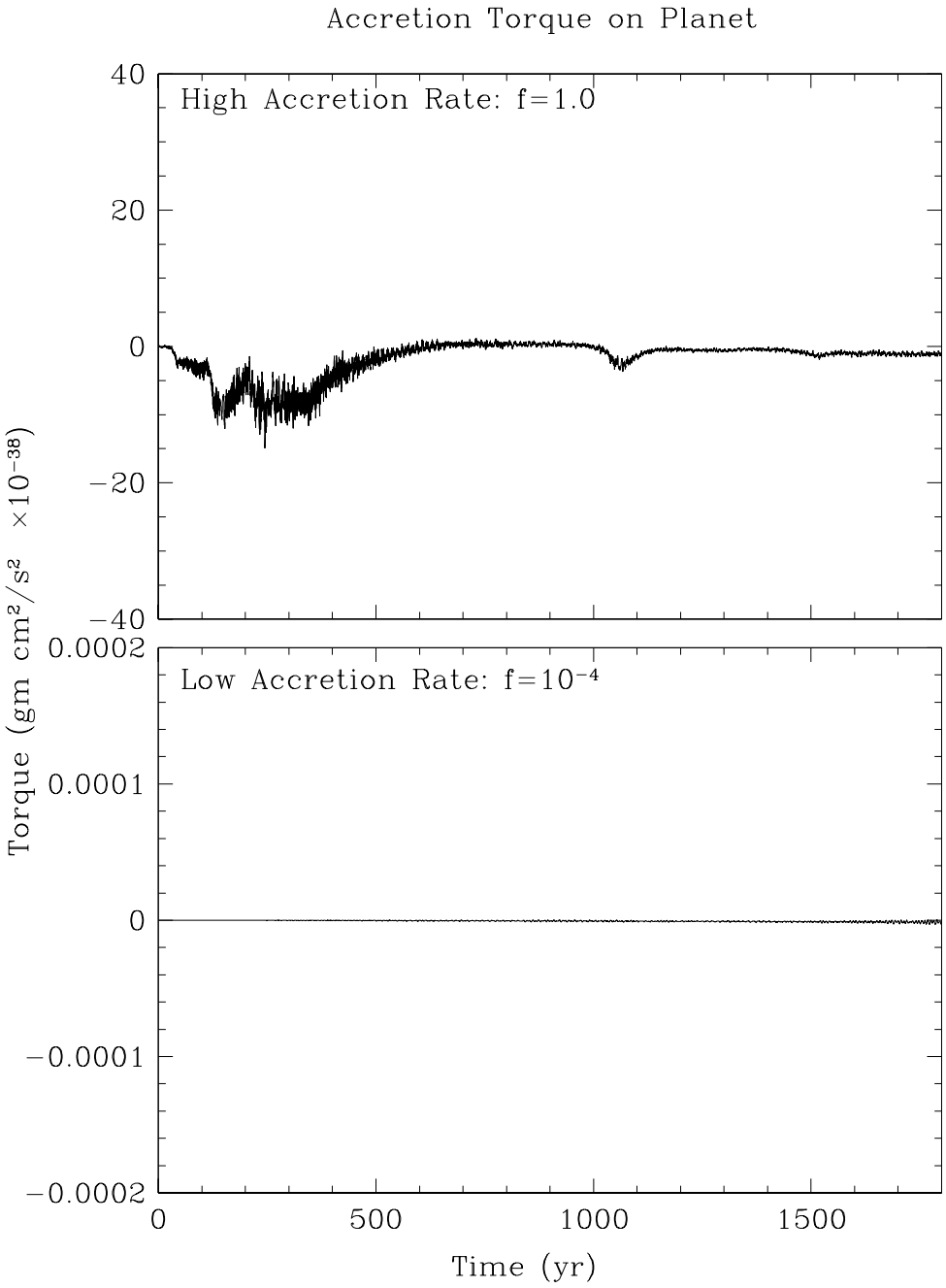

Fig. 3.— Same as figure 2, but for the models with an initial gap. Top: the torque for the initial gap model, *gap0*, with $f = 1.0$. Bottom: the torque for the $f = 0.0001$ model, *gap4*. In each case, although the magnitudes of the torques due to mass accretion are different, their signs are the same. Mass accretion provides a net, negative torque on the orbital angular momentum or the planet.

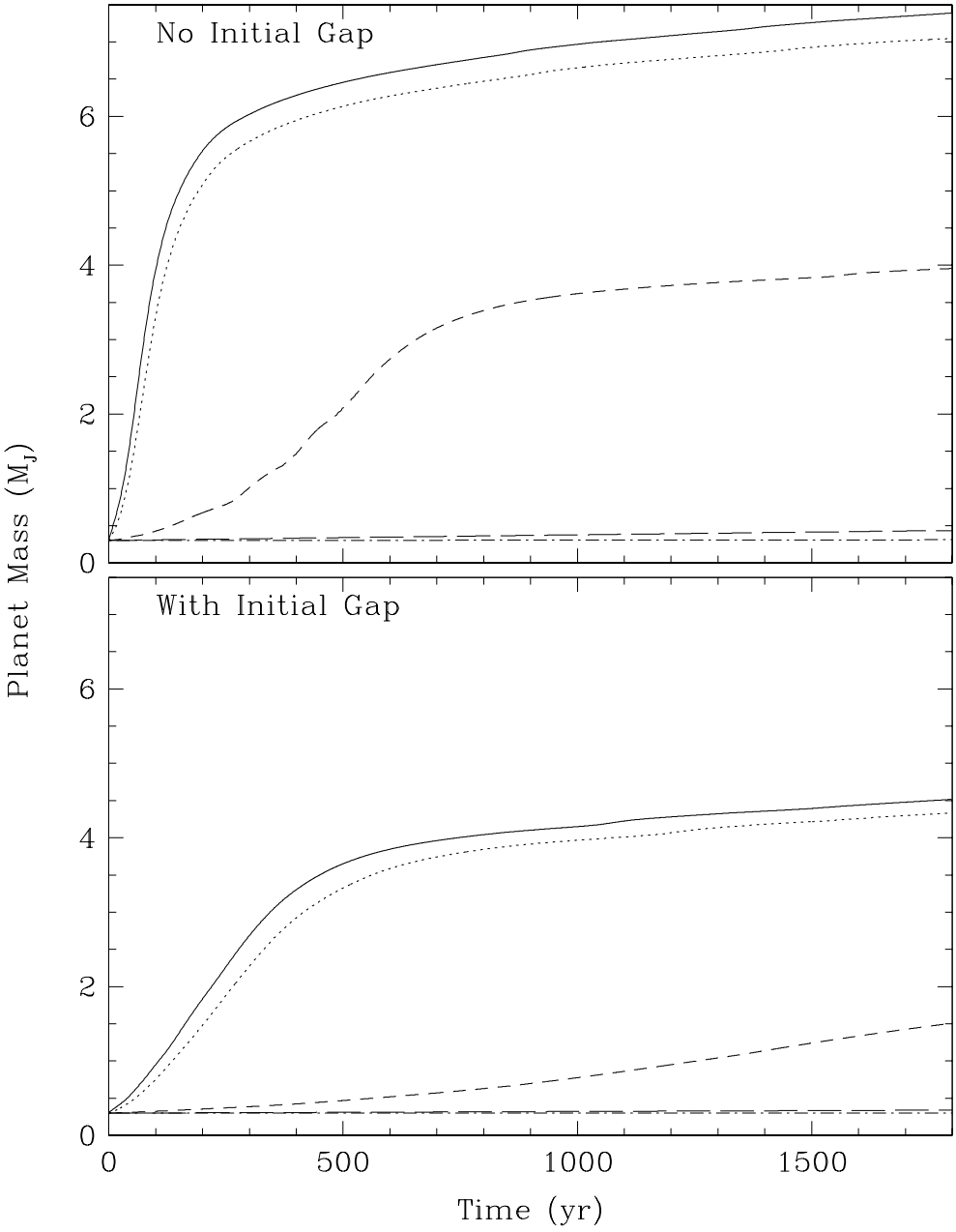

Fig. 4.— Mass of the planet as a function of time, for different assumed Bondi accretion rate fraction, f. Accretion rates defined by f =1.0, 0.1, 0.01, 0.001 and 0.0001 are shown with solid, dotted, short dashed, long dashed and dash-dotted lines respectively. In the top panel: for each of the $f > 0.001$ curves, the accretion is initially very rapid, then slows because a gap forms in the disk by virtue of the fact that all of the mass there is either accreted onto the planet, or driven to large distances from it via dynamical torques. In the bottom panel: accretion remains very rapid even in the presence of an initial gap in the disk. Again, for simulations with $f > 0.001$, the planet is able to accrete $>1 M_J$ within 1-2000 yr.

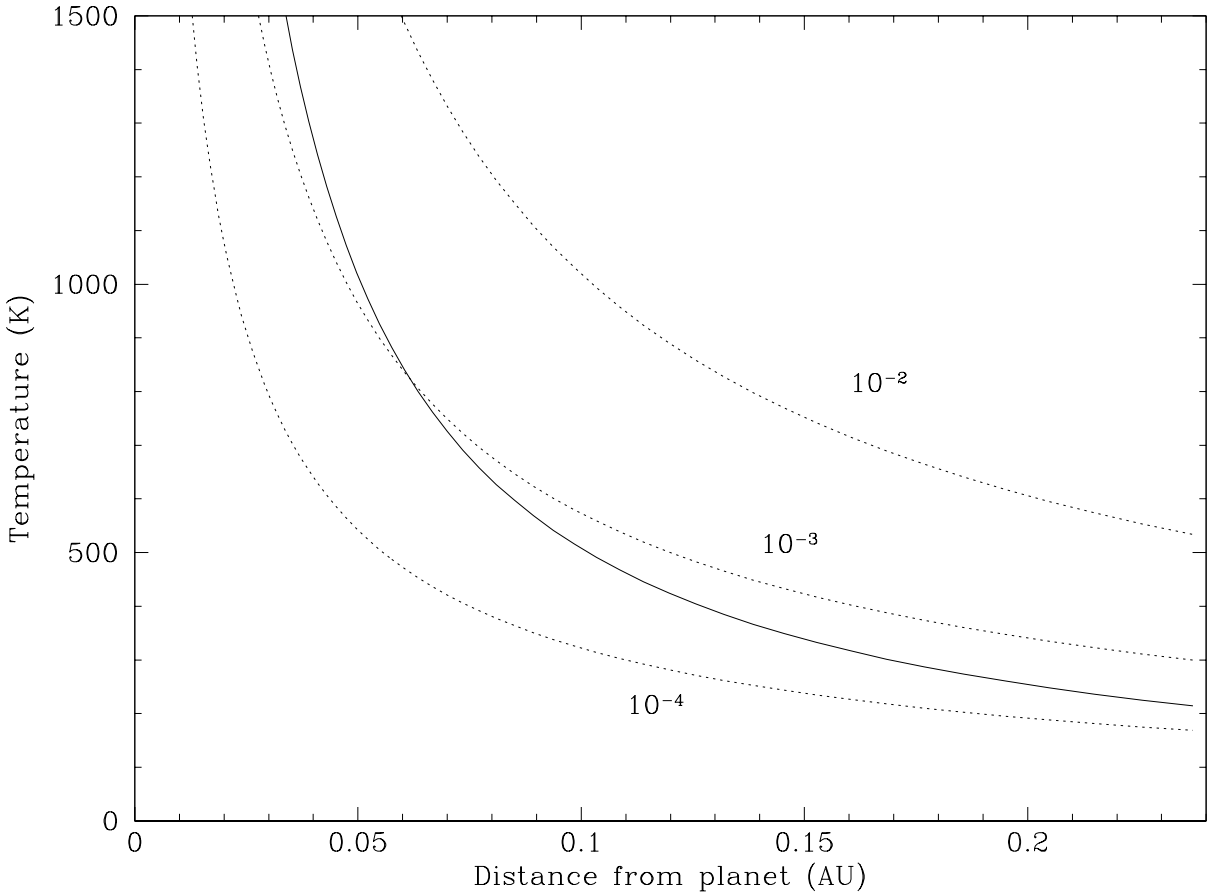

Fig. 5.— Temperature as a function of radius for an assumed steadily accreting circumplanetary accretion disk with optical depth $\tau = 100$ and various accretion rates, $\dot{M}_{\rm pl}$ (dotted curves). With this assumed optical depth, the curves correspond to accretion rates of 10^{-2}, 10^{-3} and 10^{-4} $M_{\rm J}$/yr from top to bottom. The temperature defined by the condition that $H/r = 1.0$ is also plotted with a solid curve. Only accretion rates of $\dot{M}_{\rm pl} \lesssim 10^{-4} M_{\rm J}$/yr produce temperatures which do not severely violate the condition that the disk be thin.

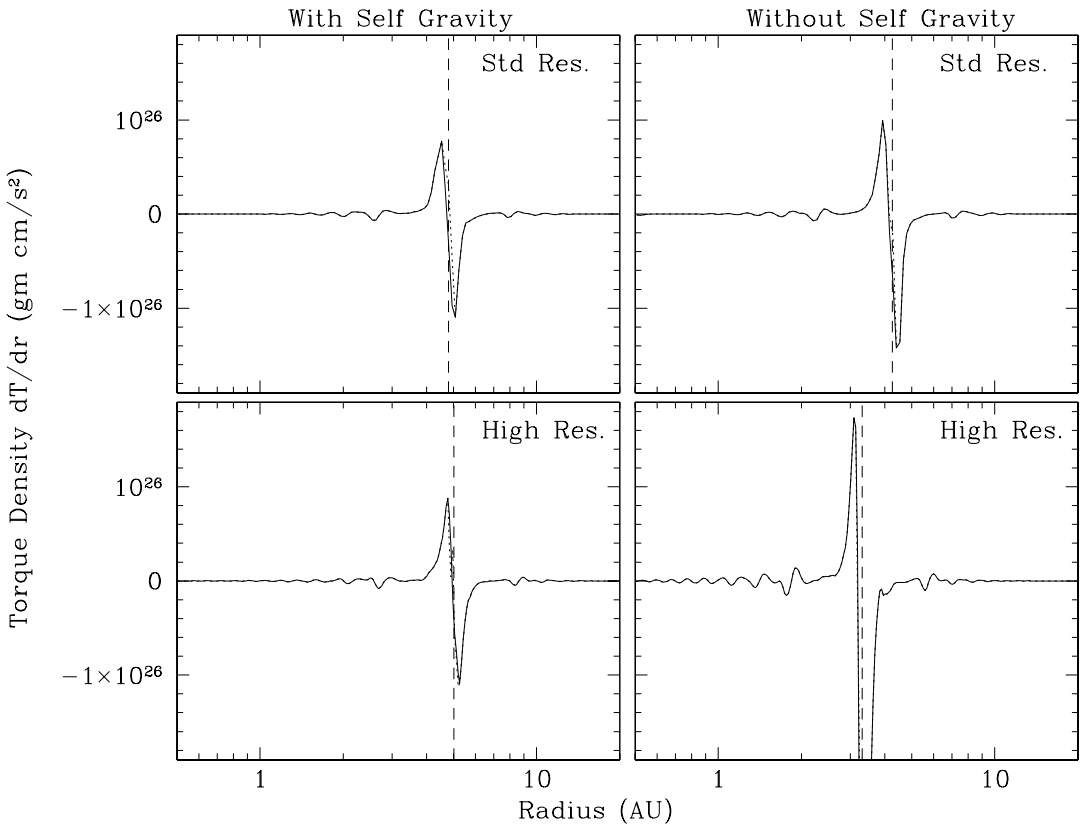

Fig. 6.— Torque density of the disk on the planet as a function of distance from the star, for the self gravitating (left) and non self gravitating disk versions of the low mass (top panels) and the high resolution (bottom panels) prototype simulations, as indicated. Each panel shows the total torque (solid line) and the total torque omitting the contribution from within the Hill sphere (i.e. within $1.0R_{\rm H}$) of the planet (dotted line). The dotted and solid lines are nearly coincident in the plot, showing that the Hill sphere itself contributes relatively little to the planet's motion. The orbit radius of the planet is shown with a vertical dashed line in each panel. The time at which the torque is evaluated is $t = 300$ yr after the initial time for each simulation.

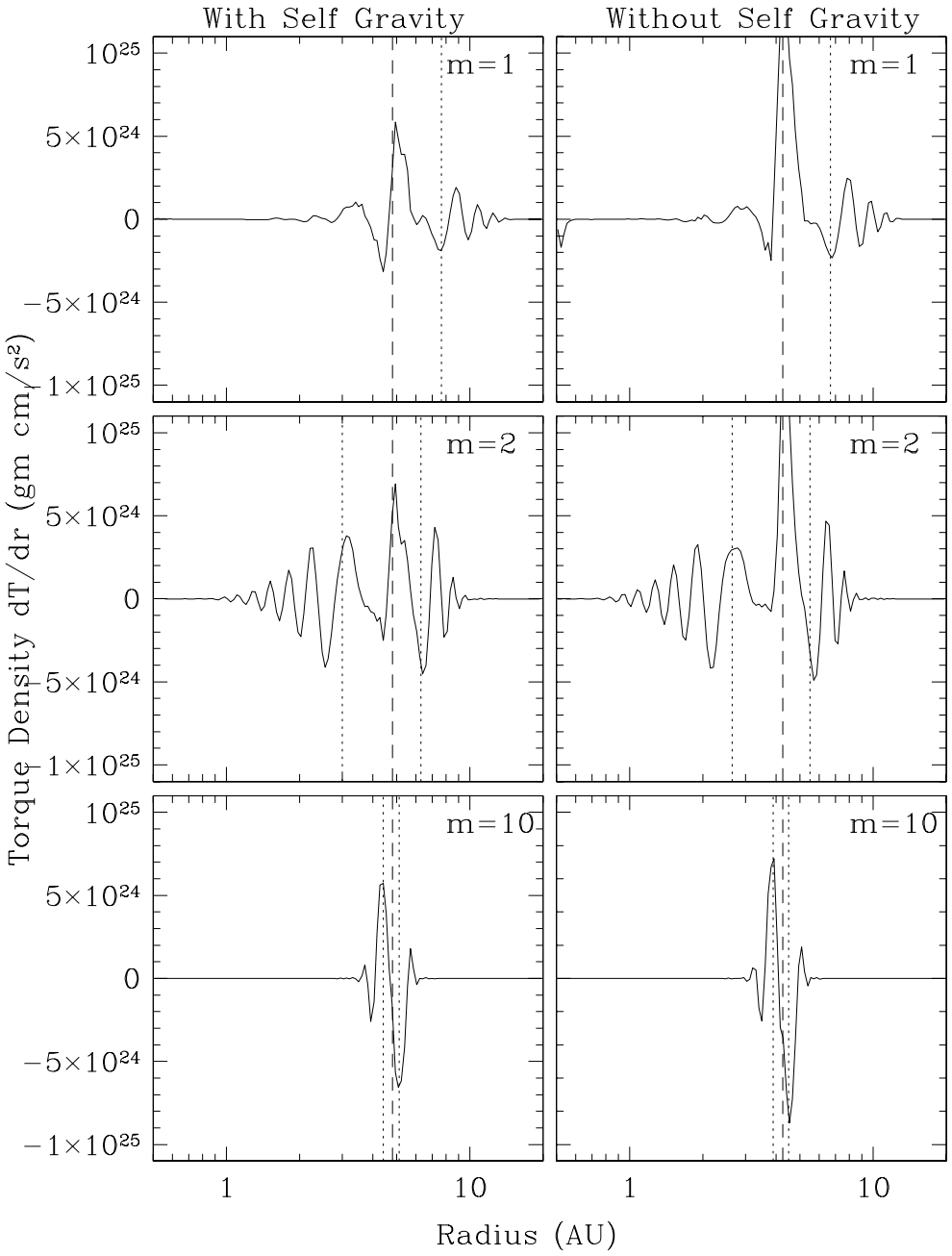

Fig. 7.— Torque density of the disk on the planet as a function of distance from the star, for the low mass prototype simulation, with (left) and without (right) disk self gravity. The three panels from top to bottom show the contributions to the torque derived from spiral patterns of $m = 1, 2$ and 10 symmetry, as marked. The orbit radius of the planet is shown with a vertical dashed line in each panel, and the Lindblad resonances with vertical dotted lines. Large torques very close to the planet are due to the corotation resonances.

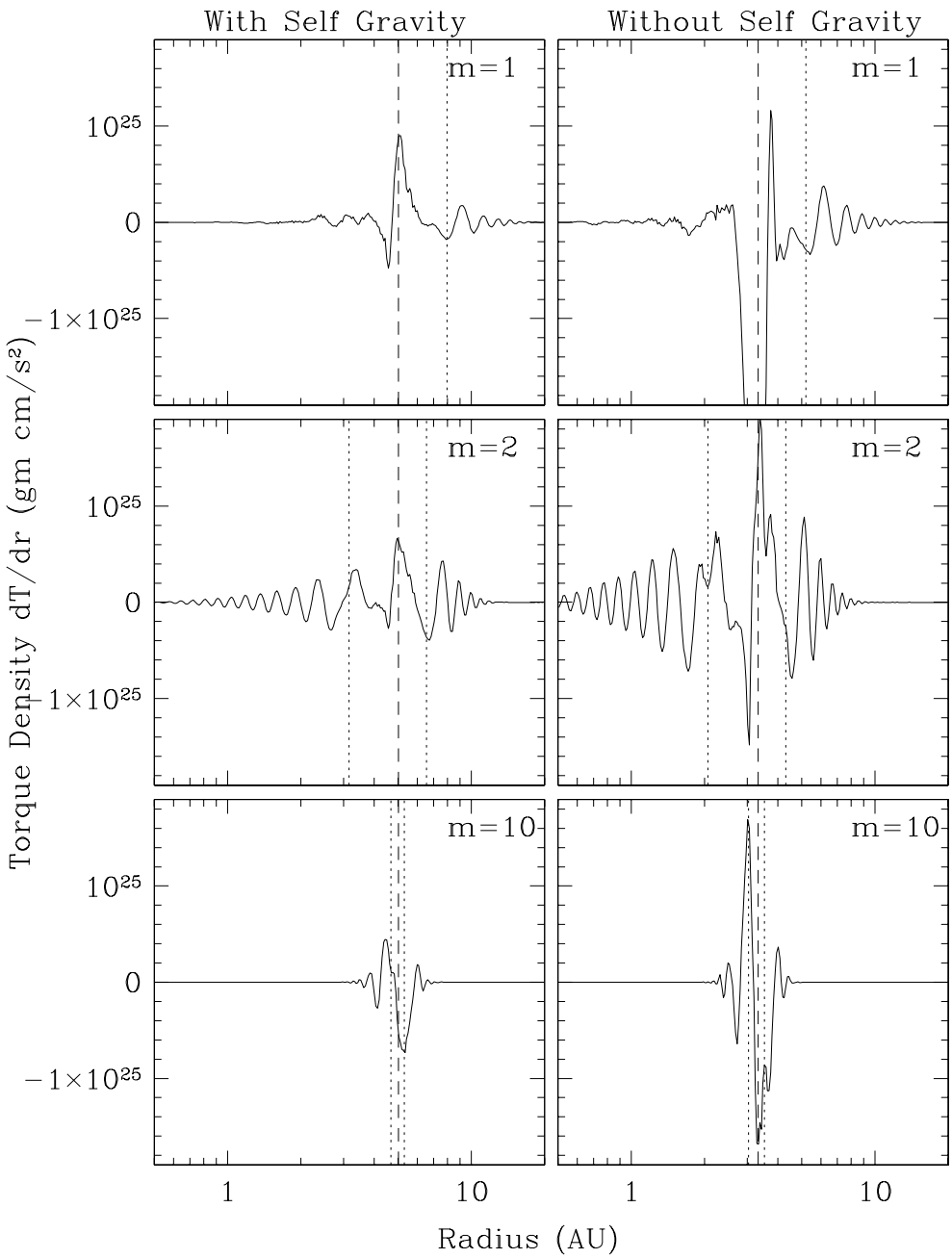

Fig. 8.— Like figure 7, except for the high resolution prototype simulations.

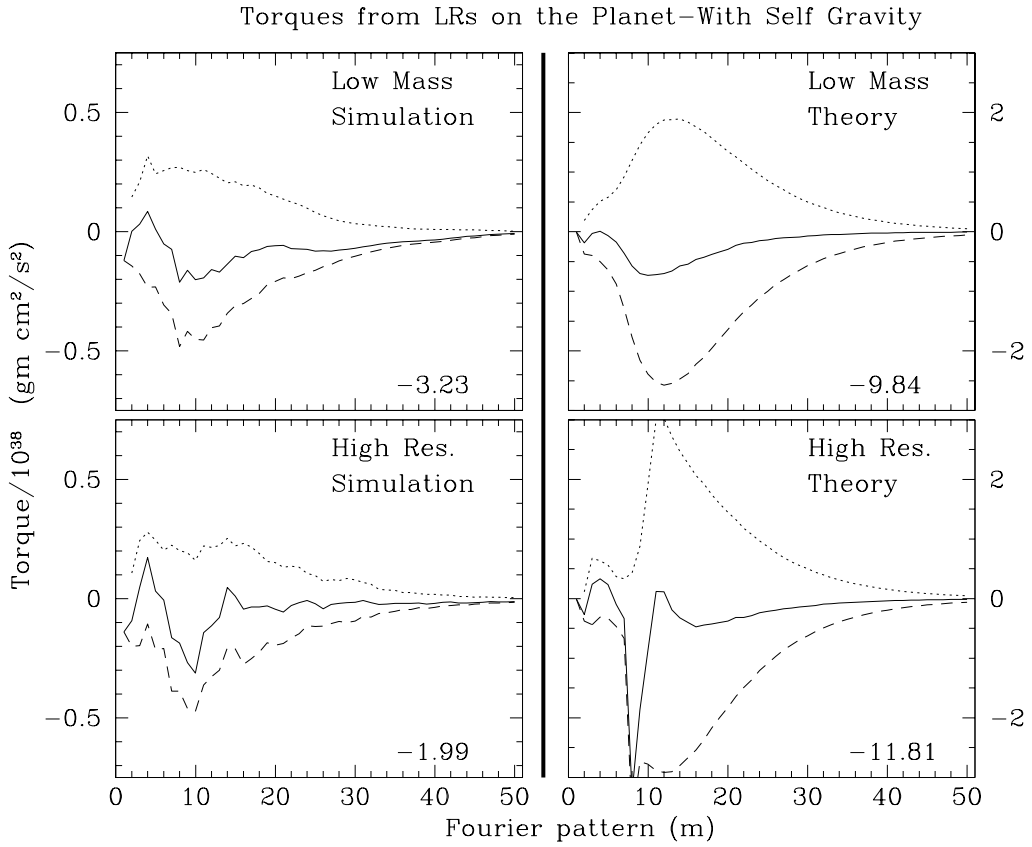

Fig. 9.— Torques of the disk on the planet generated by the Lindblad resonances with spiral symmetry m ($m \leq 50$) on the planet at time, $t = 300$ yr. As indicated, the top and bottom panels show the torques as calculated for the low mass and the high resolution prototype models. In each case, the total torque is shown with a solid line, while the torques from each ILR and OLR are shown with dotted and dashed lines, respectively. Note that the axes are expanded by a factor of four in the theory plots relative to the simulations. The number in the lower right corner of each panel is the net torque from the sum of all LRs.

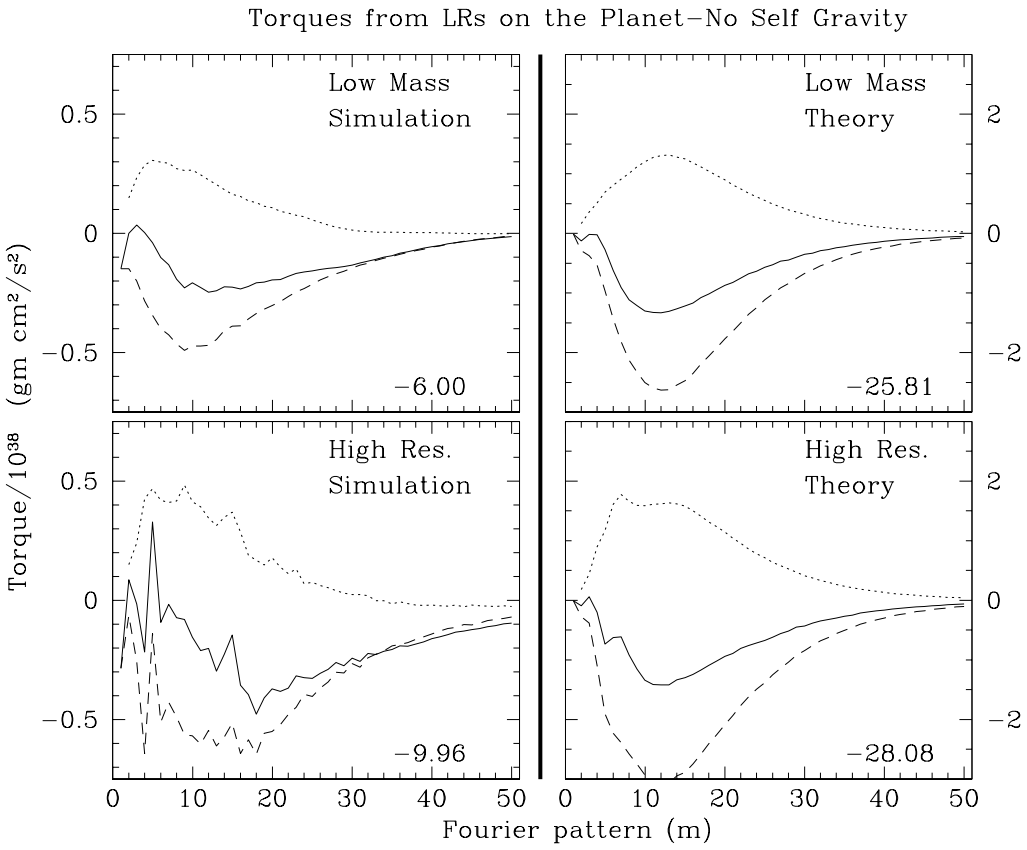

Fig. 10.— Same as figure 9, except for the simulations without disk self gravity.

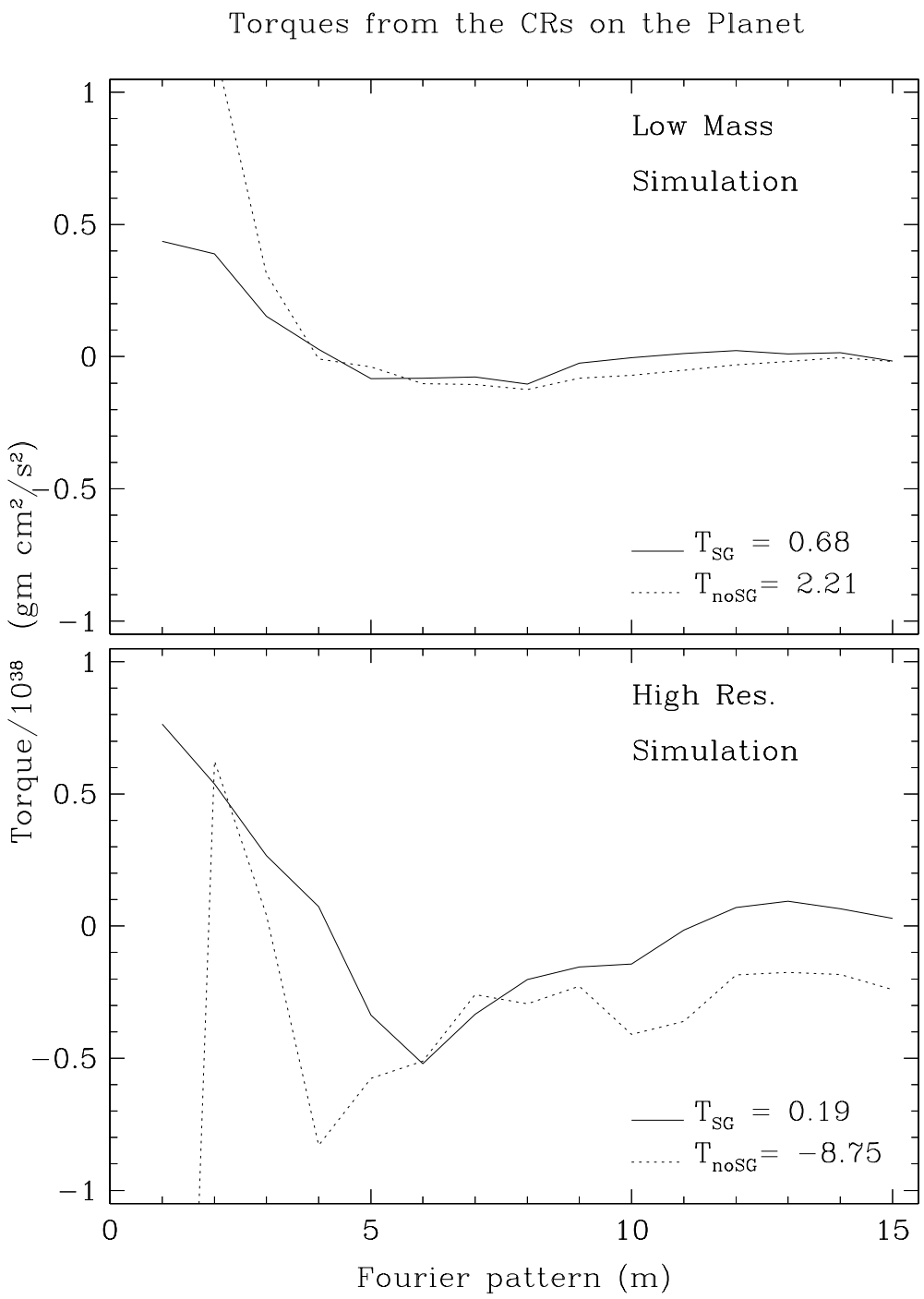

Fig. 11.— Total torques of the disk on the planet generated by corotation resonances with spiral symmetry m ($m \leq 15$), for the low mass prototype and the high resolution prototype with (solid line) and without (dotted line) disk self gravity. The net torques from the CRs are shown in the lower right corner.

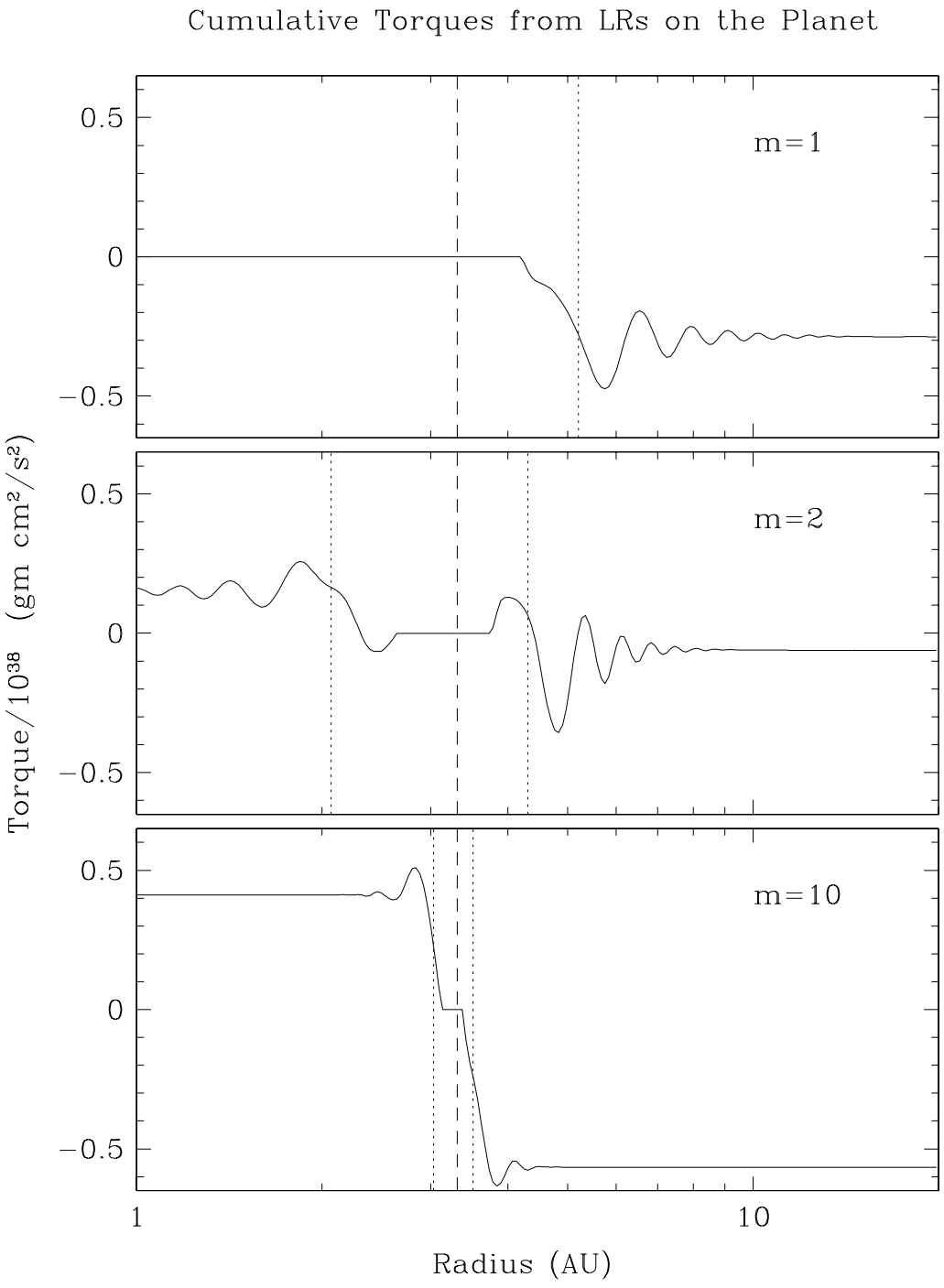

Fig. 12.— The cumulative torque from the inner and outer Lindblad resonances due to the $m = 1$, 2 and 10 patterns in the high resolution prototype simulation (without self gravity). The LR positions derived from the simulation are marked with vertical dotted lines and the planet's position is marked with a dashed line. The cumulative sum is taken as a function of distance from the planet for both the inner and outer resonances. Infinite distance inside or outside the planet's position yields the net torque from that resonance.

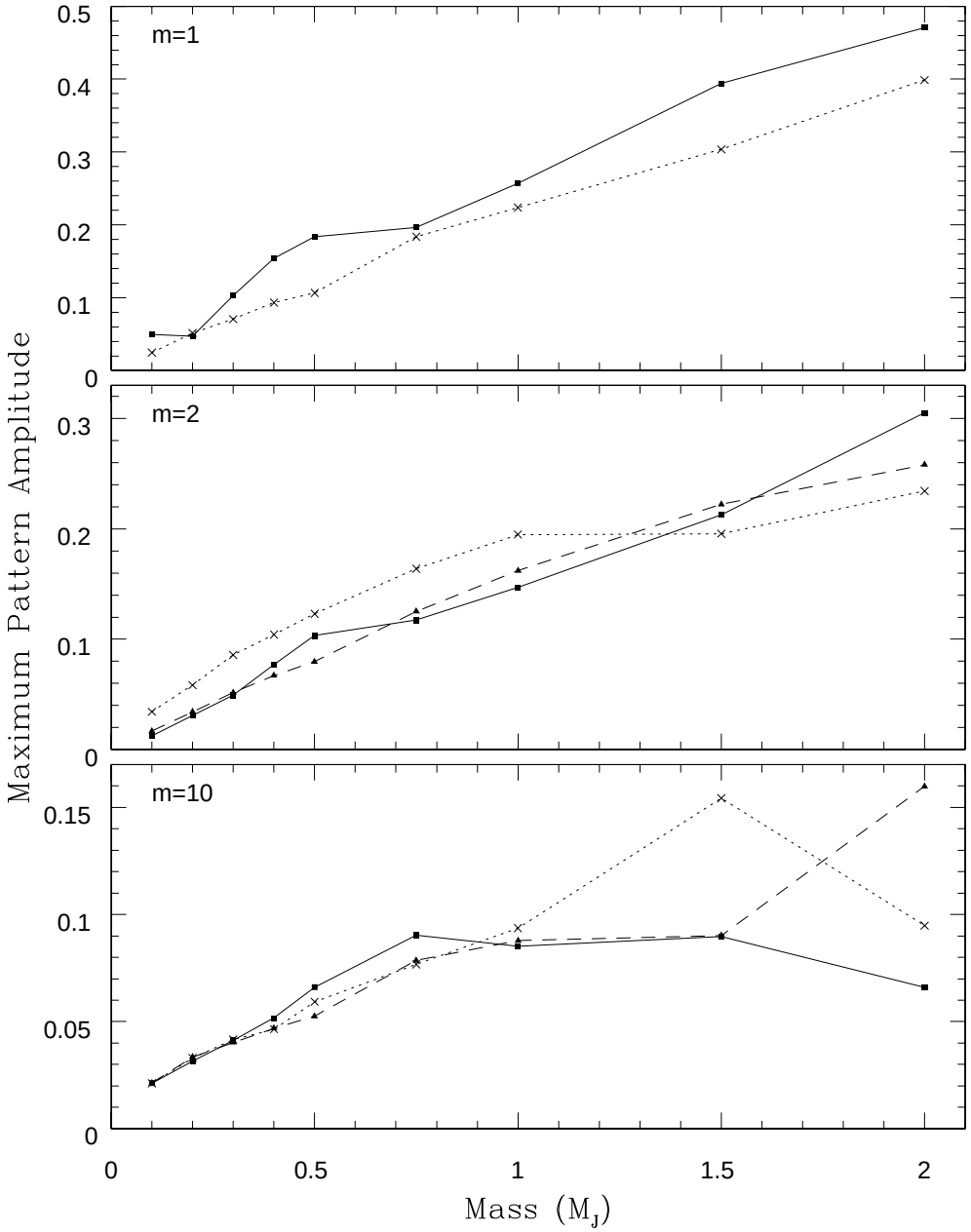

Fig. 13.— Maximum Pattern amplitudes vs. planet mass for the $m = 1, 2$ and 10 patterns between 0.1 and $2.0 M_{\rm J}$. In each plot the solid line with filled squares represents the amplitude at corotation, the dotted line with crosses ($\times$) represent the amplitude at the OLR and the dashed lines with the filled triangles represents the amplitude at the ILR. In all cases, the amplitude is normalized to the azimuth averaged surface density at the appropriate resonance.

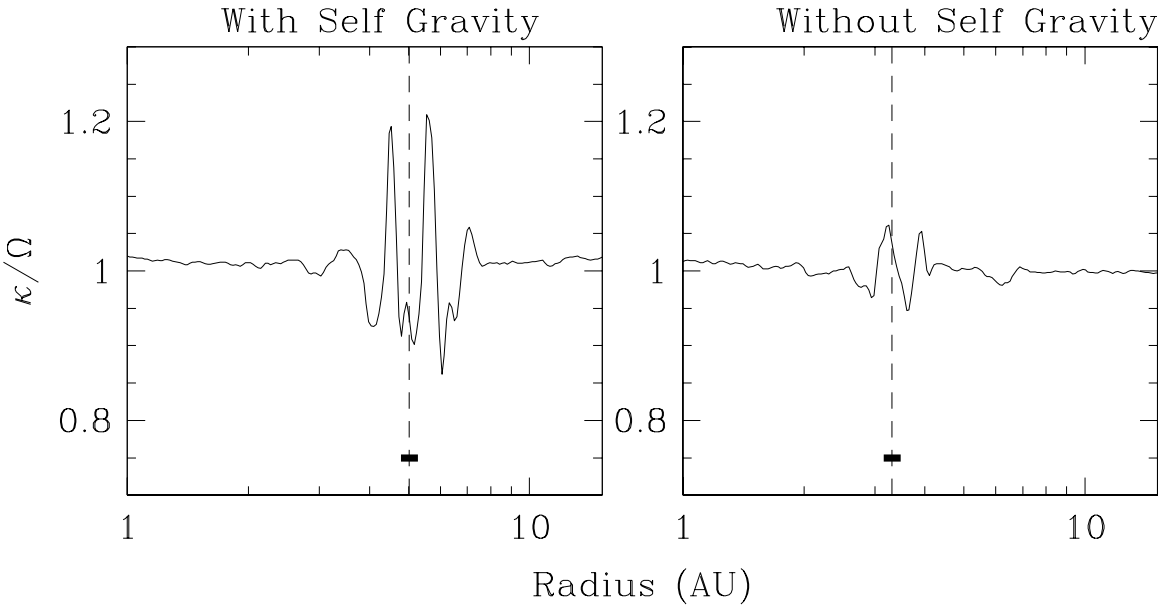

Fig. 14.— Ratio of the epicyclic frequency, κ, to the orbital frequency, Ω, at each radius for the high resolution prototype with and without self gravity, both at time $t = 300$ yr. In the gap formation region ($a_{\rm pl} \pm 4R_{\rm H}$) the quantities differ by as much as 20% due to the influence of large pressure gradients on the rotation curve. Outside the gap formation region, the ratio is near 1.02, indicating the expected near equality of the two quantities. Migration is extremely rapid in the non-self gravitating system and consequently no gap is able to form and the ratio stays near unity. In each panel, the vertical dashed line defines the position of the planet, and the thick horizontal bar defines one Hill radius around the planet.

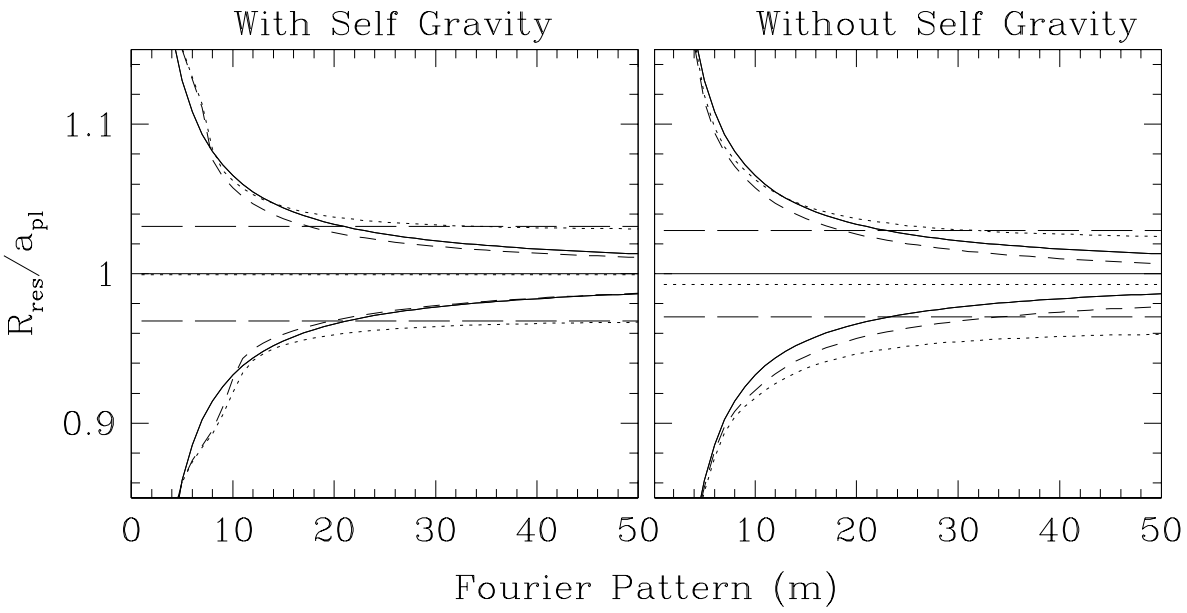

Fig. 15.— Location of the Lindblad and corotation resonances as determined from our simulations. The left and right panels show the resonance positions for the simulation with and without self gravity, respectively. The ideal Keplerian resonance positions are shown with solid lines, while the true positions (calculated using equation 8 or 9) are shown with dotted lines and the positions calculated from equation 5 are shown with short dashed lines. The horizontal long dashed lines define the extent of the buffer regions ($2H/3$) inside and outside the planet, from Artymowicz (1993a).

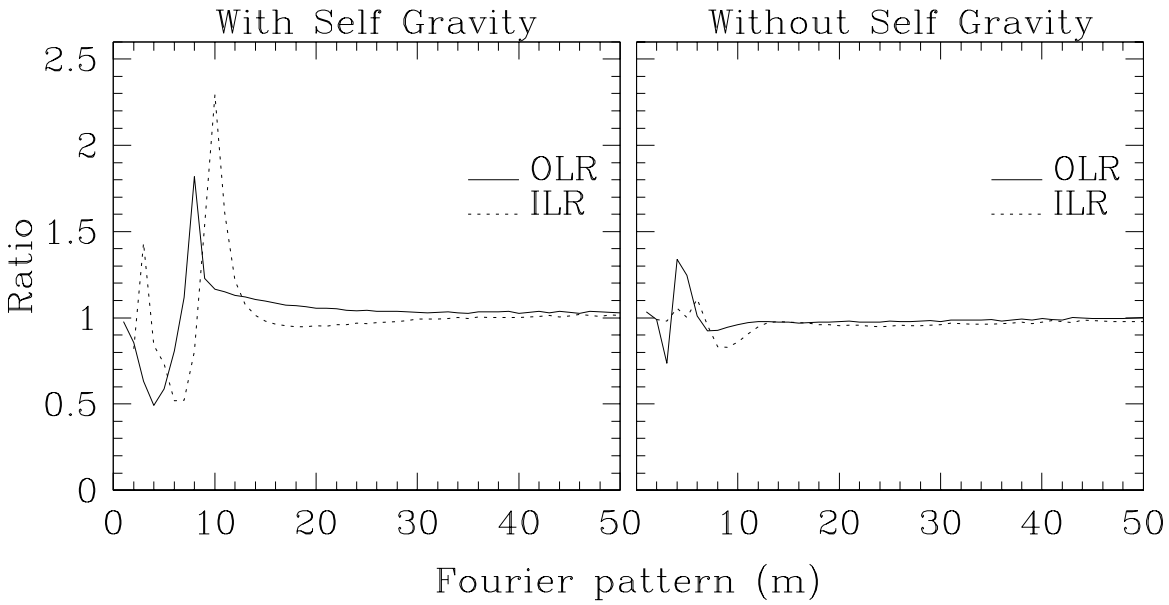

Fig. 16.— The ratio of the approximated value of the resonant denominator to the value computed numerically from the high resolution prototype simulations, with and without self gravity. The ratio is defined as $R = -3(1 \mp m)\Omega_{r_L}^2/(rdD/dr)_{num}$. As marked, the ratios at the inner resonance are shown with dotted lines while the outer resonance ratios are shown with a solid line.

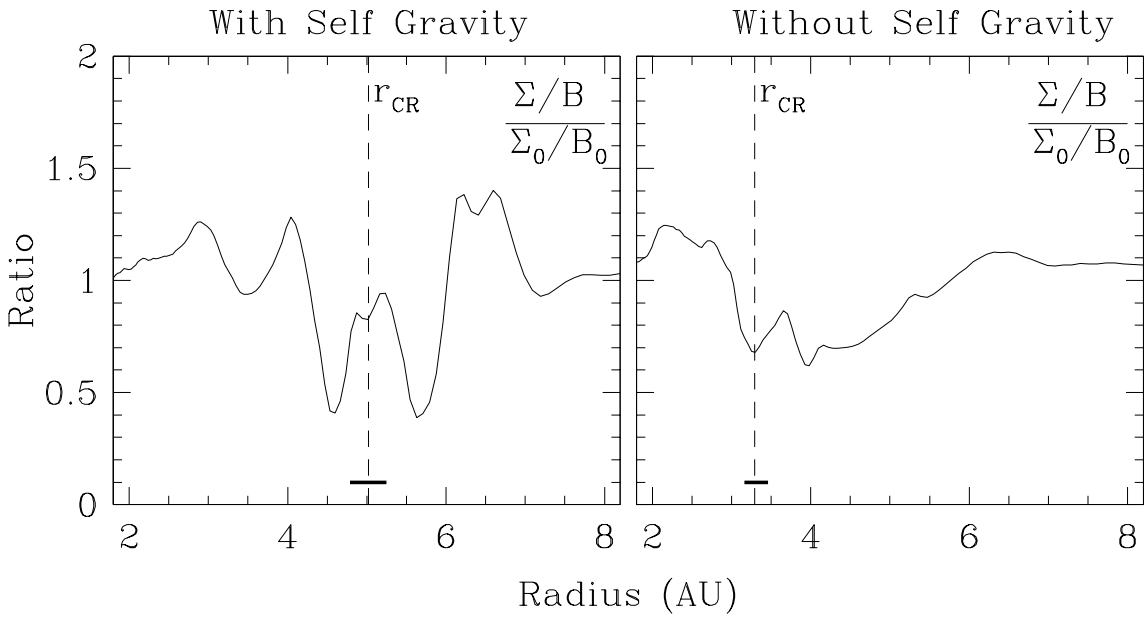

Fig. 17.— The ratio of the CR parameter Σ/B to its (near constant) initial value for the high resolution prototype simulations. The solid bar near the bottom of the plot, defines the size of the Hill sphere.

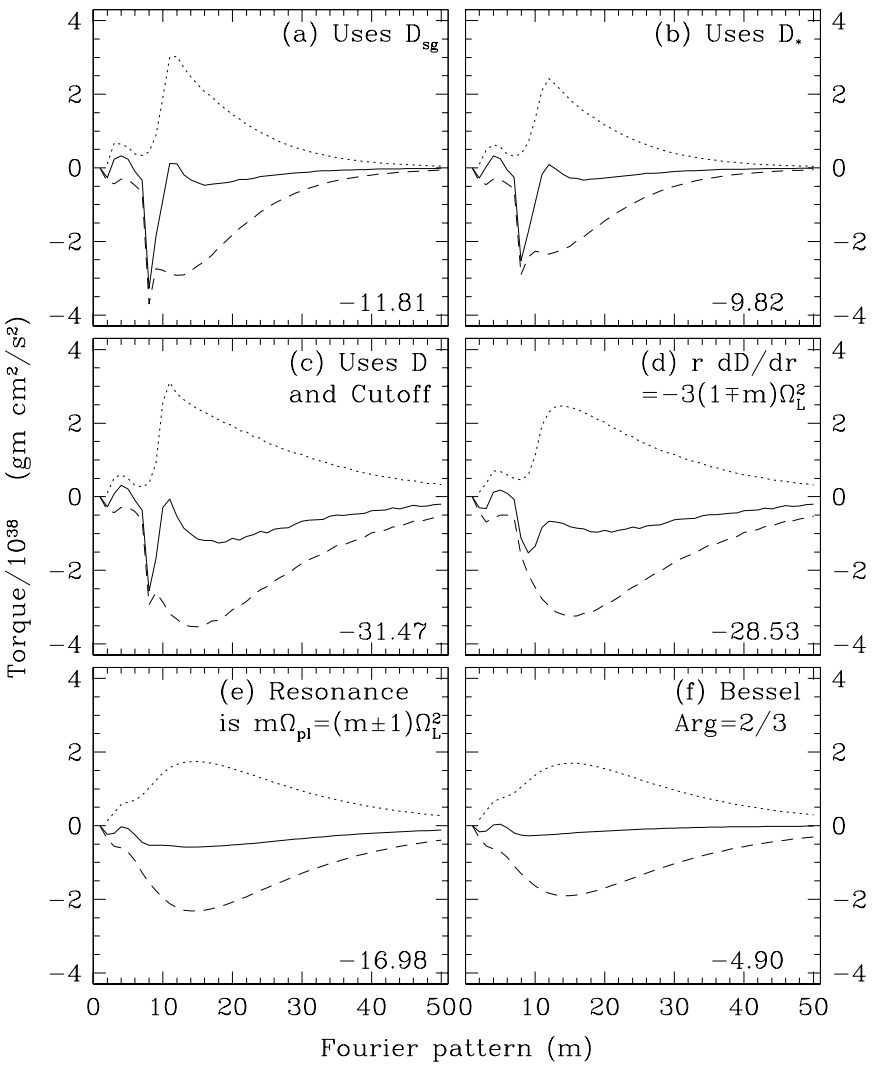

Fig. 18.— Analytic torques evaluated under various approximations to equation 4, using azimuth averaged quantities derived from the high resolution prototype at $t = 300$ yr. Successive panels (a)-(c) investigate various approximations made to the theory, while panels (c)-(f) investigate common approximations made to obtain the resonant denominator and the resonance positions. Panel (a) is a duplication of the analytic result shown in figure 9 for which the torque is calculated using the exact resonance locations, determined from D_{sg}, the generalized Laplace coefficients and the numerically determined resonant denominator, $r_L dD_{sg}/dr$. Panel (b) shows the same assumptions but with D_* replacing D_{sg}. Panel (c) replaces the combination of D_* and generalized Laplace coefficient with the combination of standard Laplace coefficients (i.e. zero softening), resonant denominator, D and the torque cutoff function, equation 6. Panel (d) Uses the approximate resonant denominator $rdD/dr|_{r_L} = -3(1 \mp m)\Omega_L^2$ rather the numerically obtained values, while retaining the numerically (from the zeros of D) obtained resonance positions. Panel (e) uses the same approximate resonant denominator, but now approximates the resonance positions to be exact integer ratios of the planet's orbit frequency. Panel (f) evaluates Bessel functions with an argument of 2/3 but uses the exact frequency ratio to define $rdD/dr|_{r_L}$. Solid, dotted and dashed curves are defined as in figures 9 and 10, above, as are the net torques shown in the lower right corner of each panel.

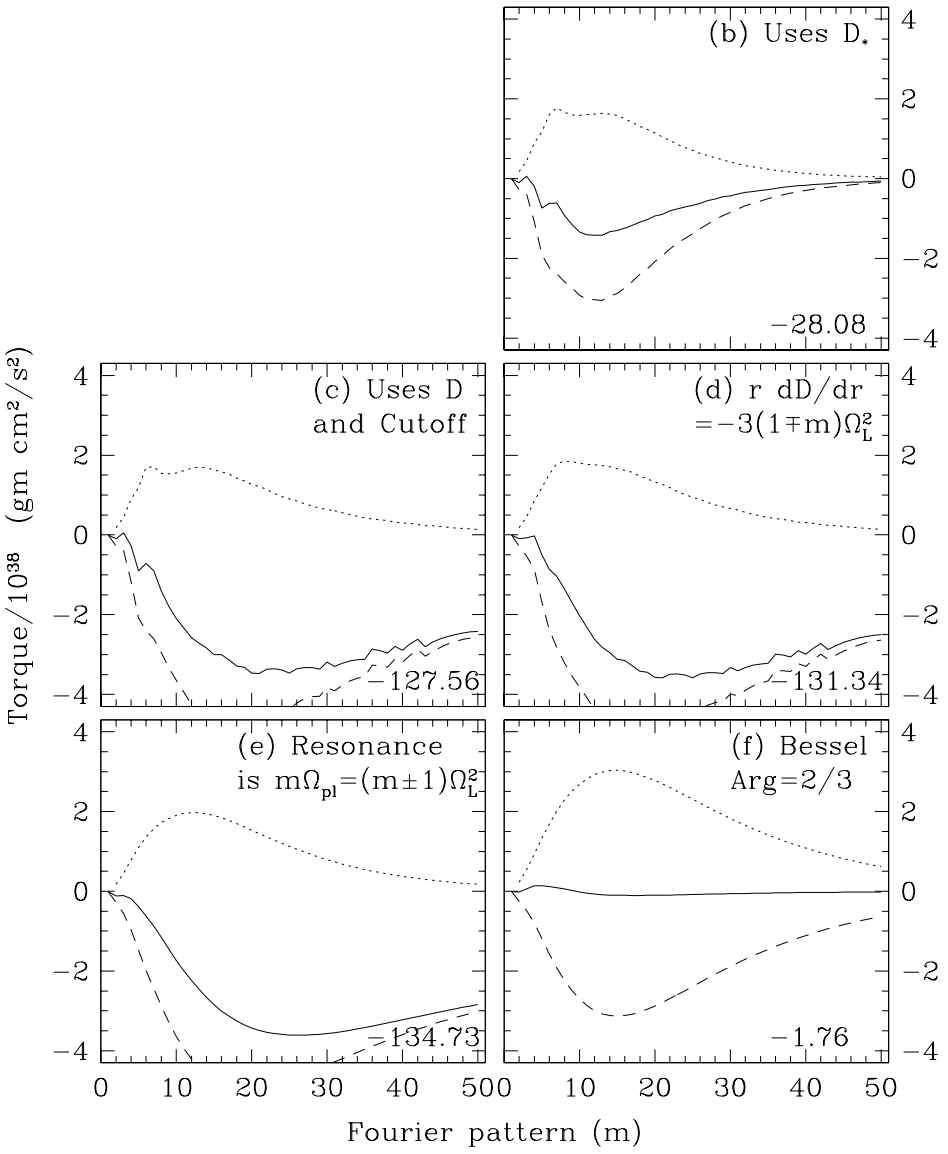

Fig. 19.— Same as figure 18, but for the non-self gravitating version of the high resolution prototype. Note that the (a) panel is suppressed because by assumption self gravity is not present in this version.

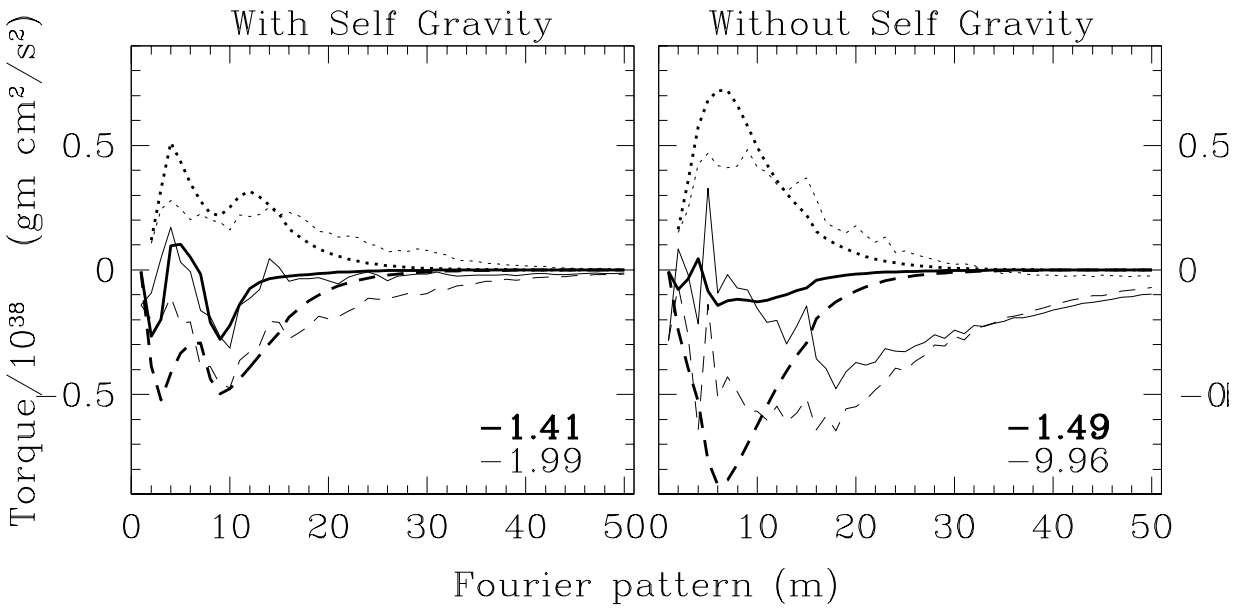

Fig. 20.— 'Best' comparison of the simulation and analytically derived torques, with and without disk self gravity. The heavy curves denote the torques from the analytic calculation, while the light curves are for the simulation. Solid, dotted and dashed curves defined as in figures 9 and 10, above, as are the values for the net torques in the lower right corner of each panel. In the generalized Laplace coefficient, we use a softening of 2.5× that in the simulation. We also use the approximation that $|rdD_{sg}/dr|_{r_L} = -3(1 \mp m)\Omega^2_{r_L}$, for $m \leq 15$.